

P60

NASA Contractor Report 182289

Improved Silicon Carbide for Advanced Heat Engines

(NASA-CR-182289) IMPROVED SILICON CARBIDE
FOR ADVANCED HEAT ENGINES Final Technical
Report (Ford Motor Co.) 60 p CSCL 11C

N91-24451

G3/27 Unclass
0019893

Thomas J. Whalen
Ford Motor Company
Dearborn, Michigan

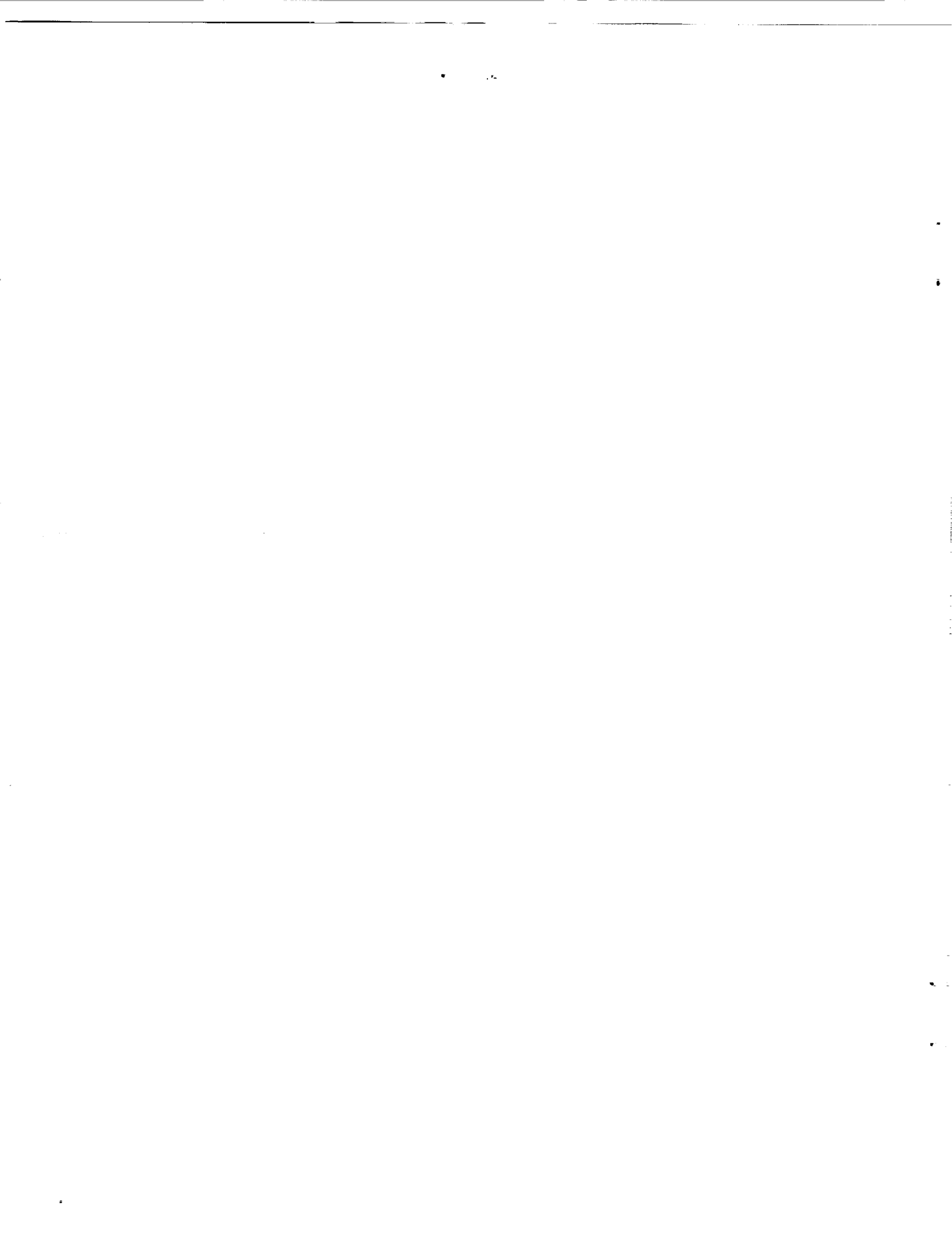
May 1989

Prepared for
Lewis Research Center
Under Contract NAS3-24384



National Aeronautics and
Space Administration

Date for general release May 1991



FOREWORD

The experimental planning, the processes of mixing, forming, dewaxing, sintering of SiC batches, the annealing, hot isostatic pressing and testing of SiC MOR bars and the analysis of data were performed by the Research Staff of the Ford Motor Company at the Scientific Research Laboratory in Dearborn, Michigan.

The principal investigator is Dr. Thomas J. Whalen. The project manager is Dr. Nancy J. Shaw of the NASA Lewis Research Center, Cleveland, Ohio. Significant contributions to this project, which commenced in February, 1985, were made by W. Trela, J. R. Baer, L. V. Reatherford, E. L. Cartwright, B. N. Juterbock, Dr. R. K. Govila, Dr. R. M. Williams (deceased), Dr. W. L. Winterbottom, Dr. S. Shinozaki and J. A. Mangels.

TABLE OF CONTENTS

EXECUTIVE SUMMARY	1
INTRODUCTION	5
TECHNICAL PROGRESS	10
1. TASK II - MOR (MODULUS OF RUPTURE) MATRIX	10
1.1 Matrix 2 Plan - Carbon Source, Carbon:Boron Ratio, Total Additives, Annealing, Hot Isostatic Pressing	10
1.1.1 Sample Preparation	10
1.1.2 Experimental Design - Density	12
1.1.3 Factorial Analysis - Density	12
1.1.4 Regression Analysis and Response Surface Modeling (Density)	12
1.1.5 Experimental Design - Strength	18
1.1.6 Factorial Analysis - Strength	18
1.1.7 Conclusions	33
1.1.8 Recommendations For Future Work	33
2 TASK VII - MATERIALS AND PROCESS IMPROVEMENTS	34
2.1 Characterization of SiC Polymorphs by Nuclear Magnetic Resonance	34
2.2 Matrix 12 Plan - Attritor Speed Optimization	39
2.2.1 Sample Preparation	39
2.2.2 Analysis of Data and Discussion of Results	39
3 TASK III - OPTIMIZED MOR (MODULUS OF RUPTURE)	42
3.1 Experimental Plan	42
3.1.1 Sample Preparation	42
3.1.2 Analysis of Data and Discussion of Results	42
CONCLUSIONS	54
REFERENCES	56

EXECUTIVE SUMMARY

This is the final technical report for the program entitled "Improved Silicon Carbide for Advanced Heat Engines" and includes the work performed during the period February 12, 1985 to December 11, 1988. The program was conducted for the National Aeronautics and Space Administration (NASA) under contract number NAS3-24384.

The objective of the program initially was the development of high strength, high reliability silicon carbide parts with complex shapes suitable for use in advanced heat engines. Injection molding was the forming method selected for the program because it is capable of forming complex parts and is adaptable for mass production on an economically sound basis. The initial goals of a 20% increase in strength and a 100% increase in Weibull modulus over the baseline properties were increased in 1987 to reflect the marked improvements made in properties. The new goals of the program were to reach a Weibull characteristic strength of 550 MPa (80 Ksi), an 86% improvement over the baseline, and a Weibull modulus of 16 (100% improvement) for bars tested in 4-point loading.

The original program included eight tasks and two of them, Task I (Baseline MOR Data) and Task VIII (Turbocharger Fabrication) were completed and reported in the first, second, and third annual reports. At NASA's direction, the two tasks involving the fabrication of large complex shapes were dropped in 1987 because of a shift in program emphasis. Three tasks are discussed in this final report; Task VII (Materials and Process Improvements), Task II (MOR Matrix) and Task III (Optimized MOR).

Many statistically-designed experiments were performed under Task VII to improve the processing of injection molded SiC and the composition of the batches. Sintered density and machined bar MOR (Modulus of Rupture) strength were the yields of these experiments.

A total of 12 experimental matrices were evaluated in Task VII. Matrices 1 through 11 were discussed in some detail in the three annual reports.

Matrix 12 was a study of the influence of the rotational speed of the attritor (mixer), which is used in the fluid mixing process, on the density and strength of the MOR bars. The results of this study clearly indicated that increasing attritor speed produced a statistically significant improvement in mechanical strength. The beneficial effect of increased attritor speed is believed to be a result of the improved homogeneity of the fluid-mixed batches.

Task II (MOR Matrix) involved two iterations of a 2^{5-1} designed experiment in which 5 factors were evaluated at two levels each. The first iteration dealt with the processing variables: mixing modifications, % solids, dewaxing conditions, sintering temperature and time. The results were presented in the Second Annual Report.

The second iteration of Task II is presented in this final report. The five factors evaluated at two levels each were the source of carbon, the

carbon:boron ratio, the total amount of carbon and boron, with and without annealing and with and without hot isostatic pressing. The yields of the experiment were density and strength. It was found that carbon added as carbon black is superior to carbon added as resin, that a carbon:boron ratio of 6:1 is better than 2:1, that 3% additives is better than 2%, and that annealing and hot isostatic pressing are beneficial to strength.

Task III (MOR Optimization) was carried out with three batches of identical material which were processed according to the best results of the twelve matrices in Task VII and the two matrices in Task II. The batches were fluid mixed in the attritor at high speed, 460 RPM, injection molded at low pressure, dewaxed in vacuum, sintered in vacuum to 1760 °C, argon sintered to 2120 °C for 30 minutes, and annealed in air at 1200 °C for 18 hours. Half of the samples were hot isostatically pressed at 207 MPa (30 Ksi) argon pressure at 1950 °C for 30 minutes. Proof testing at 586 MPa (85 Ksi) was performed to study the effect on the Weibull modulus.

For groups of 60 bars of each of the 3 batches, Weibull characteristic strengths in excess of 592 MPa (86 Ksi) with a Weibull modulus of 8 were attained. By proof testing, a Weibull modulus greater than 16 was measured for each of the three batches. Strengths were also measured at 1400 °C and found to be the same as those measured at room temperature. Hot isostatic pressing of the MOR bars did not improve the strength of these Task III materials. The goals of the program were exceeded by the MOR bars produced under Task III.

A summary of the mean MOR strengths attained with the baseline material and with the process and material improvements during the duration of the program is shown in Figure 1.

Magic angle spinning nuclear magnetic resonance spectra of SiC polymorphs were used to characterize the powders and follow the polymorphic transformations that occurred during the sintering of SiC. The initial spectra of the beta SiC powder is that of a broad single peak which transforms to three peaks on sintering of the powder to a dense solid, indicative of the alpha polymorphs. Magic angle spinning nuclear magnetic resonance may be the most sensitive method for characterizing and quantifying the polymorphs of SiC during processing.

Molding yields, defined as the percentage of void-free or inclusion-free molded bars, were determined and shown to improve significantly over the course of the program. These data were reported in the Third Annual Report.

The distributions of the numbers of flaws observed visually and by x-radiography on samples of molded and sintered MOR bars were shown to be approximated by a Poisson distribution. These data were in the third annual report.

Statistical process control was used throughout the program for the mixing, molding, dewaxing and sintering processes. Examples of these control charts and their use were given in the three earlier annual reports.

IMPROVED SILICON CARBIDE FOR ADVANCED HEAT ENGINES (INJECTION MOLDED) NAS 3 - 24384

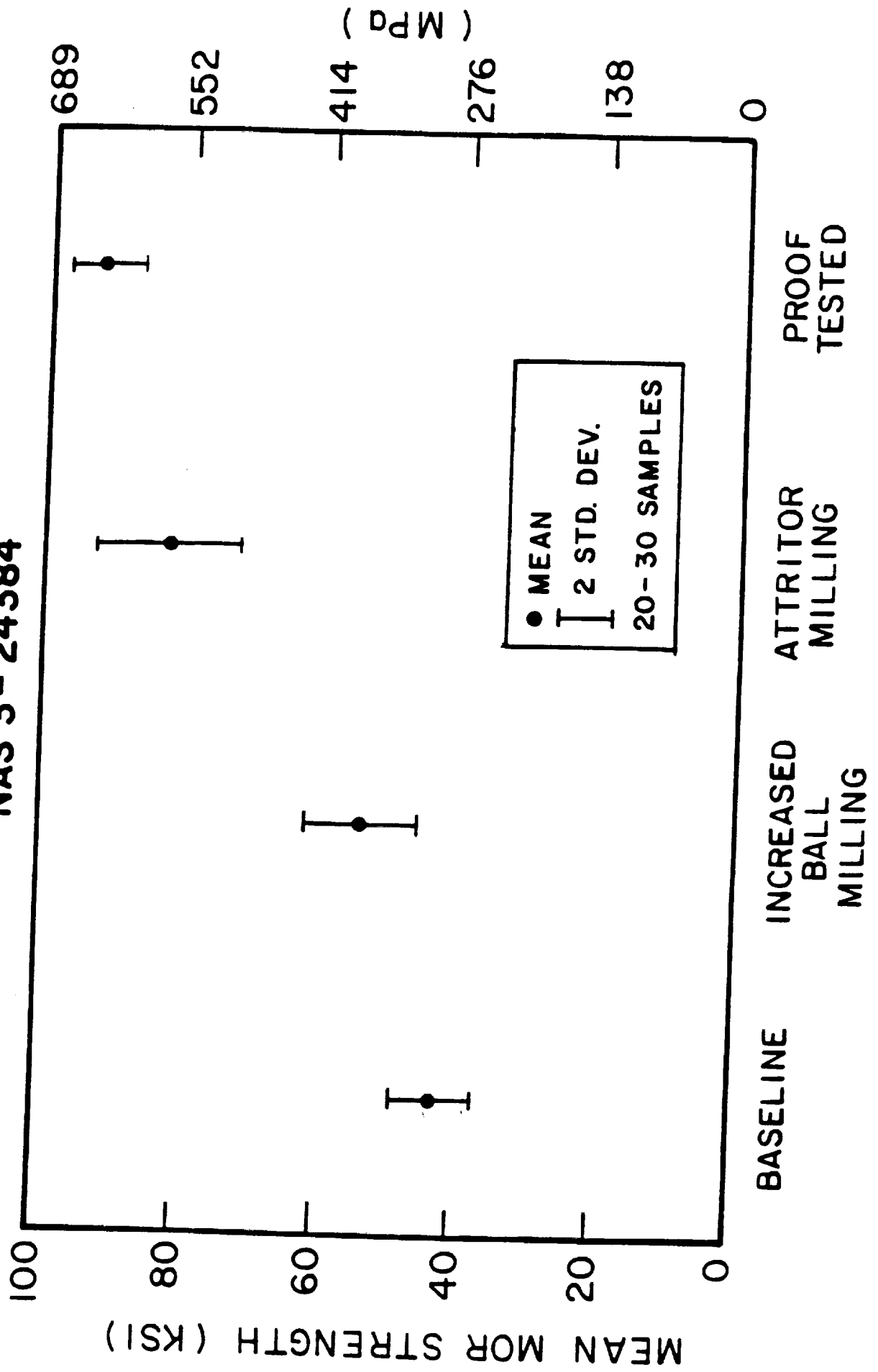


FIGURE 1

FLUID PROCESS IMPROVEMENTS

The results obtained in this program demonstrated that the strength and density of the MOR SiC bars produced can be adequately represented by a normal distribution and normal statistical tests are applicable. With large sample sizes (>30 bars) a Weibull distribution was found to be adequate. Statistical tests were used for each case to verify the assumptions. Outliers are usually present in data sets of strength, and we have observed that on the average, 2 bars per 100 are outliers for normal, or Weibull distributions, regardless of considerable efforts to use nondestructive tests to separate potential outliers. The processing and quality control at this stage of development is at the 98% yield level.

It has been shown in this program that proof testing can provide improved reliability (increased Weibull modulus or decreased standard deviation).

Conclusions:

Strength improvements of 87% in MOR and 100% in Weibull modulus (with proof testing) were attained by using statistically-designed experiments to improve processing and compositional variables which led to the reduction of flaw sizes.

Sintered densities were improved from 94% to 99% of theoretical density.

Annealing of MOR bars in air significantly increased strength.

Strength measurements at 1200 °C and 1400 °C were the same as room temperature strength. These materials may be the strongest, stable materials at 1400 °C in air which can be formed into complex shapes.

Magic angle spinning nuclear magnetic resonance was found to be a powerful tool in determining silicon carbide polytypes present in both the starting powders and the sintered samples.

INTRODUCTION

This is the final technical report on the program entitled "Improved Silicon Carbide for Advanced Heat Engines" submitted by the Ford Motor Company. The program is conducted for the National Aeronautics and Space Administration (NASA) under contract number NAS3-24384. This report covers the period February 12, 1985 to December 11, 1988.

The objective of this program was to develop high strength, high reliability silicon carbide material, with the potential to form complex shapes suitable for advanced heat engines components. The fabrication method was to be adaptable to the mass production of complex parts on an economically sound basis.

The final revised program schedule is given in Figure 2. The program contains the fabrication, evaluation and improvement of test bars of size 3 X 6 X 51 mm and was divided into five Tasks:

Task I - Fabricate and characterize the baseline silicon carbide material. The results, shown in the first annual report (Ref. 1), were a characteristic strength of 316 MPa (45.8 Ksi) with a Weibull modulus of 8. The mean strengths at room temperature, 1000⁰ C, 1200⁰ C and 1400⁰ C were 299 MPa (43.3 Ksi), 285 MPa (41.4 Ksi), 298 MPa (43.2 Ksi) and 325 MPa (47.2 Ksi) respectively.

Task II - Improve silicon carbide MOR test bars with process and material improvements by iterative, statistically-designed experiments. Two groups of experiments were performed as a half-fraction of a 2⁵ design which permitted evaluation of main effects and two-factor interactions. The details of the experiments were reported in the second annual report (Ref. 2). One group was vacuum sintered while the second group was argon sintered. The five variables which were evaluated at two levels each were Process A (fluid mixing) and Process B (modified fluid mixing with improvements), solids loading (55% and 60%), dewaxing process (argon and vacuum), sinter time and sinter temperature. For both the argon sintered and the vacuum sintered groups, Process B was significantly better than Process A, and, for the vacuum sintered group, the shorter sintering time of 6 minutes was better than 12 minutes. The other variables did not significantly influence the strength, but some variables did influence the sintered density.

The best group of 8 duplicate MOR bars from the vacuum sintered matrix had a mean strength of 444 MPa (64.5 Ksi) and a standard deviation of 70 MPa (10.1 Ksi). The best group of 30 vacuum-sintered bars had a mean strength of 423 MPa (61.4 Ksi) with a Weibull characteristic strength of 442 MPa (64.2 Ksi) and a Weibull modulus of 10.5. The best group of 28 argon-sintered bars had a Weibull strength of 407 MPa (59.1 Ksi) and a Weibull modulus of 10.1. The strength of the vacuum-sintered material is 40% greater and the Weibull modulus is 31% greater than those values measured for the baseline material in Task I.

The second iteration of Task II will be discussed in this report in the Technical Progress section.

SIC Program Timing Chart

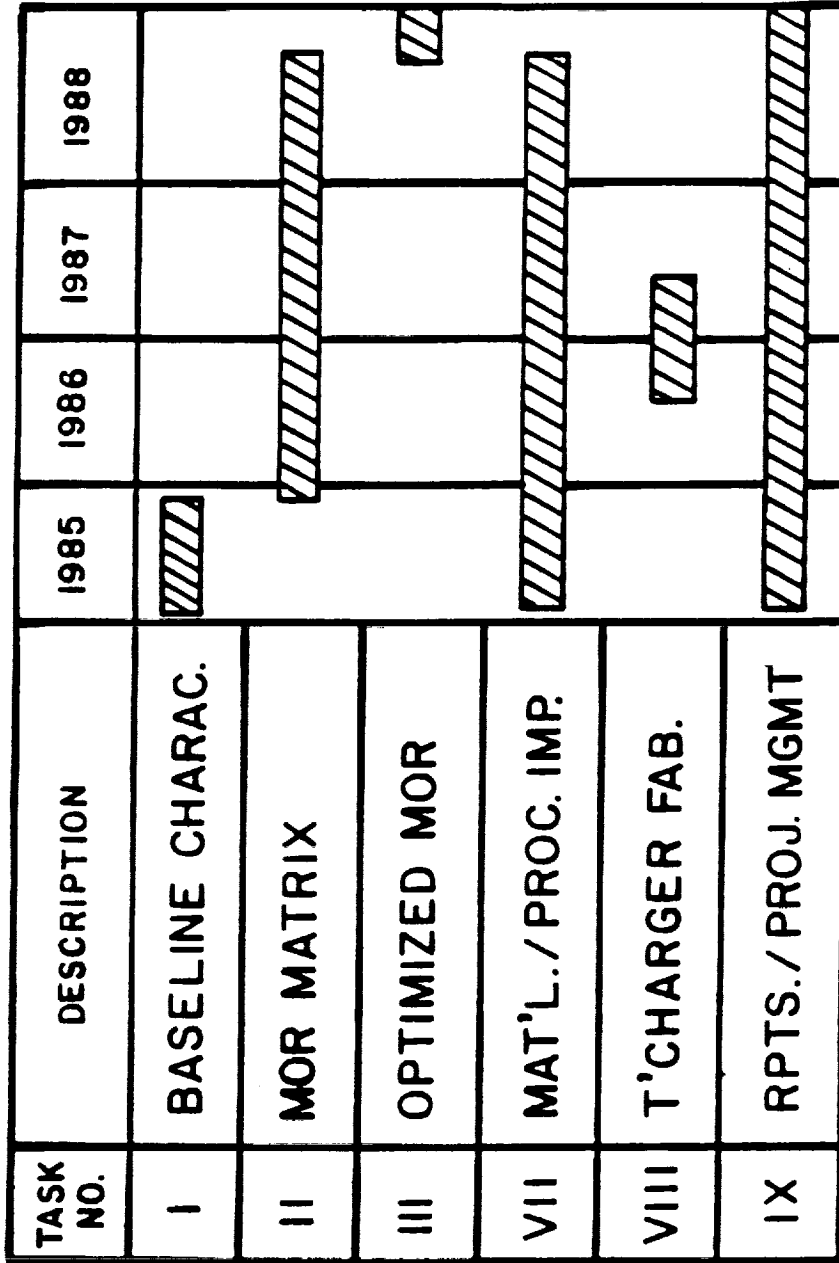


FIGURE 2

Task III - Characterize the improved process and material. The details of Task III work will be presented in the Technical Progress section of this report.

Task VII - Advance silicon carbide technology with statistically-designed experiments and input these advances into Tasks I, II, and III. Twelve matrix experiments were performed under Task VII and these are summarized as follows:

Matrix 1 - Baseline Composition - A 2^3 factorial experiment was performed to select the baseline composition. The 3 factors were SiC powder source, carbon source and solids loading level and the yield was sintered density. It was determined that the SiC source should be Ibiden ultrafine (UF) powder, that carbon should be added as carbon black, and that the higher loading level was better. Details of this work can be found in Ref. 1.

Matrix 2 - Dewaxing Cycle - A 2^2 factorial experiment was carried out with heating rate and pressure as the two factors and sintered density as the yield of the experiment. The sintered density was found to be the same for all four conditions and, based on availability of equipment and cost, a heating rate of 5^0 C per hour in vacuum was chosen for the dewaxing process for the baseline material (Ref. 1).

Matrix 3 - High-Shear Processing - Dry mixing procedures were found to be inadequate for use with the ultra-fine powders, since agglomerates and other inhomogeneities were not effectively reduced. A sampling procedure was developed and used as a control parameter for the mixing process. Several high-shear mixing procedures were evaluated and it was found that the Haake Mixer was the most satisfactory. This procedure was used for the baseline material (Ref. 1).

Matrix 4 - Fluid Mixing Process - A mixing process was developed by dissolving the molding waxes in toluol, mixing in the SiC and additives in a ball mill, and removing the toluol by evaporation. This procedure greatly reduced the agglomerate size and led to improvements in density and strength (Ref. 1).

Matrix 5 - Argon Sintering - The baseline sintering process was carried out in vacuum. A low-density case around each sample suggested that dissociation of the SiC was occurring. A 2^2 factorial experiment was performed to evaluate sintering in an argon atmosphere, with sintering temperature and heating rate as the two factors and sintered density as the yield. Acceptable densities were found and further studies were planned (Ref. 1).

Matrix 6 - Dewaxing Cycle Factors - A 2^{5-2} fractional factorial experiment was performed to evaluate the effect of 5 factors at 2 levels each on the dewaxing process in 8 experimental runs. The 5 factors were gas type (nitrogen or argon), gas pressure, temperature, holding time, and heating rate. The yield of the experiment was percent of wax removed during dewaxing. There were significant effects of temperature and pressure and a temperature-pressure interaction on the amount of wax removed (Ref. 2).

Matrix 7 - Vacuum-Argon Sintering Cycle Factors - A 2^{4-1} fractional factorial design was used to study 4 factors at 2 levels each for the effect on density and strength. The 4 factors were backfill temperature, time of hold before backfill, heating rate, and material composition. The significant effects on density were backfill temperature, time of hold before backfill, and material composition. The effects on strength were less significant than on density, but the same factors appeared to influence the strength (Ref. 2).

Matrix 8 - Fluid Mix Process, Carbon Source and Sintering Parameters - A 2^{7-4} fractional factorial design was chosen to study the main effects of 7 factors at 2 levels each in 8 runs. The factors were fluid mixing process (A and B), carbon source (DeGussa carbon or carbon black), argon heating rate (9 or 5⁰ C/Min.), sintering temperature (2080 or 2120⁰ C), sintering hold time (12 or 30 Min.), backfill temperature (1620 or 1760⁰ C), and vacuum hold time (4 or 2 hr). For density, the significant factors were mixing process, sinter temperature and time, and backfill temperature. For strength the significant factors were mixing process, sintering time and backfill temperature (Ref. 3). The results of this matrix study supplied the sintering conditions for the remaining work on this program.

Matrix 9 - SiC Powder Source and Boron Level - A 2^2 design was chosen to study the effects of 2 powder sources (Ibiden and Superior Graphite) and 2 boron levels (0.5% and 1.0%) on the density and strength. For density the Ibiden powder sintered to a higher density than the Superior Graphite powder, and the higher boron content sintered to a higher density. For strength, neither effect was significant (Ref. 3). At this point in the program we had two sources of SiC powder that would be satisfactory.

Matrix 10 - Annealing Study - A 2^2 factorial design was used for the annealing study with 2 factors, temperature and atmosphere, at 2 levels each. The 2 temperatures were 1200⁰ C and 1400⁰ C (for 18 hr.) and the two atmospheres were air and argon. For strength the air atmosphere was significantly better than argon and the lower temperature was significantly better than the higher one (Ref. 3). At this point in the program we added the annealing process to the fabrication process.

Matrix 11 - Attritor Process Study - a 2^3 factorial design was employed to study 3 factors at 2 levels each. The 3 factors were batches mixed in an attritor mixer, sintering runs, and with and without annealing. For density, the analysis showed that the attritor batch 2 was higher than attritor batch 1, indicating the importance of slight changes in attritor mixing procedure. Annealing at 1200⁰ C significantly decreased the density over that of the unannealed material. This decrease in density is believed to be a result of forming a lower-density oxide skin on the bars. For strength, the attritor batches and the sintering runs had no effect but the annealing treatment had a strong, significant effect (Ref. 3). Oxidation of the surface may reduce the harmful effects of surface imperfections and improve strength by a crack blunting process. The annealing process may also reduce detrimental residual stresses

produced from machining of the bar surfaces, which would also improve the strength of the bars.

Matrix 12 - Attritor Speed Optimization Study - This study is treated in some detail in the Technical Progress section of this report.

Task VIII - Form a turbocharger rotor from the best material and process available to supplement the information developed during the other tasks with simpler shapes and to provide preliminary data for the Tasks which were planned for large complex shapes, and which were later cancelled. Ford supported Task VIII as a cost-sharing effort. Results are given in Ref. 2 and include a molding study of the turbocharger rotor. A 2^{5-1} fractional factorial experiment was performed in which 5 molding factors or variables were evaluated at 2 levels each. The molding variables were injection pressure, die temperature, material temperature, flow rate, and time at pressure. The yields of the experiment were density, volume and number of cracks observed at 7X magnification. The significant effects were: for density, the material temperature; for volume, injection pressure and material temperature; and for cracks, die temperature with several two-factor interactions. Three molding conditions were found to yield crack-free molded rotors. No further work was done on these molded rotors.

During the first year of the program a guiding principle was developed from observations of the fracture surfaces and extensive microstructural analysis in the transmission electron microscope and the scanning electron microscope (Ref. 1). Quite clearly, the strength of the material was controlled by the size, shape and location of the flaws or agglomerates introduced during the early processing step of mixing. Since the strength of brittle materials generally follows the Griffith equation, the strengths observed in this program also were explained by the Griffith relation. A discussion of the relationship between agglomerate size, flaw size and strength was given in Ref. 1.

During the fourth year of the program, which is discussed in this report, the major effort was centered on the second iteration of the matrix in Task II (MOR Matrix) - Matrix 2, Task VII - Matrix 12 (Attritor Speed Optimization Study) and Task III (Optimized MOR).

TECHNICAL PROGRESS

1. TASK II - MOR (MODULUS OF RUPTURE) MATRIX

1.1 Matrix 2 Plan

Numerous two-factor factorial and fractional factorial experiments were performed to evaluate the parameters in the processing steps cited above (Ref. 1,2,3). It was found that the dewaxing, sintering, annealing and hot isostatic pressing steps were well controlled and that the strength variations introduced by these steps were very small. It was also known that the strength was influenced primarily by the flaws introduced during the processing step of mixing and that the nature and amount of the additive content contributed to the size of the flaws (References 1, 2, 3).

It was the purpose of this experiment to determine the effects of five factors at two levels on the density and strength of the silicon carbide bars. These five factors were carbon:boron ratio, total amount of carbon and boron, carbon source, annealing, and hot isostatic pressing (HIP).

1.1.1 Sample Preparation

The Ford process contains the following steps:

- Fluid mix the silicon carbide powder in the attritor mill with additives of boron, carbon and molding wax;
- Remove the fluid by heating in a controlled environment;
- Mix additional molding wax if required;
- Injection mold test bars to produce finished bars of 3 X 6 X 51 mm;
- Dewax the molded bars in a vacuum environment;
- Sinter the bars in an inert environment;
- Hot Isostatic Press (HIP), in some cases, to improve density and/or strength;
- Inspect and machine bars to the final dimensions;
- Inspect machined bar surfaces;
- Anneal the machined bars to improve strength;
- Measure density by a water immersion technique and strength in a four point bending test;
- Inspect fractured surfaces for fracture origin.

MOR bars were molded from the ten batches prepared by the attritor process. An analysis of the density of the molded bars indicates that a linear regression model can be developed to adequately represent the density data. The data, shown in Table I, fall into two different groups, one for the density of molded bars with carbon added as lampblack and the other with carbon added as resin. The dependent variable of the linear model, the molded density, is given by a constant and two predictors, weight percent boron and weight percent carbon in the mixes.

For the molded bars with carbon added as lampblack:

$$Y = 2.22 - 0.00699 X_1 - 0.0133 X_2 \quad (R^2 \text{ adjusted} = 75.3\%)$$

TABLE I
 MOLDED DENSITIES OF MOR BARS
 FOR TASK II MATRIX 2 STUDY

<u>BATCH NUMBER</u>	<u>WT %</u> <u>C</u>	<u>WT %</u> <u>B</u>	<u>MEAN MOLDED</u> <u>DENSITY (g/cc)</u>	
<u>Carbon Source</u>			<u>LAMP BLACK</u>	<u>RESIN</u>
1	1.3	0.7	2.1977	2.0846
2	2.0	1.0	2.1848	2.0631
3	1.7	0.3	2.1926	2.0740
4	2.6	0.4	2.1815	2.0514
5	2.0	0.5	2.1933	2.0705

and for the bars with carbon added as resin:

$$Y = 2.12 - 0.00578 X_1 - 0.0261 X_2 \quad (R^2 \text{ adjusted} = 94.3\%)$$

where Y - density in g/cm³
X₁ - weight % boron
X₂ - weight % carbon

Several statistical tests were carried out which confirmed that these linear models adequately represent the data.

1.1.2 Design of Experiment (Density)

Task II Matrix 2 was originally designed as a 2⁵⁻¹ fractional factorial experiment with 5 factors in 16 experiments with 2 additional facepoints. To consider the sintered density only, three factors have been used so that the design can be simplified to a 2³ full factorial as shown in Table II. The three factors and their levels are listed in Table III, batch compositions in Table IV and the results of the experiment in Table V.

1.1.3 Factorial Analysis (Density)

The average effect on density for the 3 factors and their interactions are listed in Table VI. Normal probability plotting of these effects (see Figure 3) shows that only the A and B factors (C:B Ratio and Total % C + B) have a significant effect on density. This is seen in the Figure by the large distances that the points at A and B are from the normal probability line (estimated best fit through small-effects data). The other factors are closely grouped about the line. Other analytical tests also confirm that the factors A and B are the significant factors influencing the density. This is seen in the plot of the residuals when the effects of factors A and B are removed from the data. Figure 4 shows the normal probability plot of the residuals and the data are seen to be adequately represented by a straight line (least squares fitted line).

1.1.4 Regression Analysis and Response Surface Modeling (Density)

Two regression models have been determined using the individual density data and dividing the data into two groups, one with carbon black as the source of carbon and the second with the resin as the carbon source. Division of the data in this way leads to a reduction in sample variance and improved regression models. After investigating several transformations of the data, the best linear fit is obtained with the natural log of the inverse of the carbon content and natural log of the boron content for the data with carbon black materials. For the density data from the resin materials, a good linear fit is obtained with the inverse of the carbon content and the boron content. For carbon content in the range of 1.3 to 2.6% and boron content in the range 0.3 to 1.0%:

$$Y = 2.994 - 0.050 / \log X_1 - 0.036 \log X_2 \quad \text{for carbon black batches} \\ R^2 \text{ (adjusted)} = 95.0\%$$

$$Y = 3.267 - 0.580 / X_1 - 0.103 X_2 \quad \text{for resin batches} \\ R^2 \text{ (adjusted)} = 95.3\%$$

Table II
2³ Full Factorial Design (+ 2 facepoints)

A	B	C	
-	-	-	
+	-	-	
-	+	-	
+	+	-	
-	-	+	
+	-	+	
-	+	+	
+	+	+	
0	0	-	facepoint
0	0	+	facepoint

Table III
Task II/Matrix 2 Factors & Levels

Factor ID	Factor Name	Levels		
		-	0	+
A	Carbon/Boron Ratio	2:1	4:1	6:1
B	Total% Carbon+Boron	2	2.5	3
C	Carbon Source	Carbon Black		Resin

Table IV
Task II/Matrix 2 Batch Compositions

Batch #	Ratio C:B	Total% C+B	Carbon %	Boron %	
1&6	2:1	2	1.3	.7	
3&8	6:1	2	1.7	.3	
2&7	2:1	3	2.0	1.0	
4&9	6:1	3	2.6	.4	
5&10	4:1	2.5	2.0	.5	facepoints

TABLE V

TASK II - MATRIX 2

RESULTS: % DENSITY OF MACHINED BARS

<u>RATIO C:B</u>	<u>TOTAL % C+B</u>	<u>CARBON SOURCE</u>	<u>BATCH #</u>	<u># OF BARS</u>	<u>AVERAGE %DENSITY</u>
2.1	2	C.BLACK	1	60	88.9
6.1	2	C.BLACK	3	60	92.8
2.1	3	C.BLACK	2	57	92.1
6.1	3	C.BLACK	4	60	93.8
2.1	2	RESIN	6	60	86.5
6.1	2	RESIN	8	59	91.5
2.1	3	RESIN	7	60	90.7
6.1	3	RESIN	5	59	94.2
4.1	2.5	C.BLACK	9	30	93.4
4.1	2.5	RESIN	10	30	93.4

TABLE VI

TASK II - MATRIX 2
AVERAGE EFFECT OF FACTORS ON % DENSITY

<u>FACTOR ID</u>	<u>FACTOR NAME</u>	<u>AVERAGE EFFECT</u>
A	RATIO C:B	3.521
B	TOTAL % C+B	2.815
C	CARBON SOURCE	-1.164
AB	interaction	-.902
AC	interaction	.740
BC	interaction	.708
ABC	interaction	.163
avg	average	91.303

Task II/Matrix 2
Normal Probability Plot of Effects

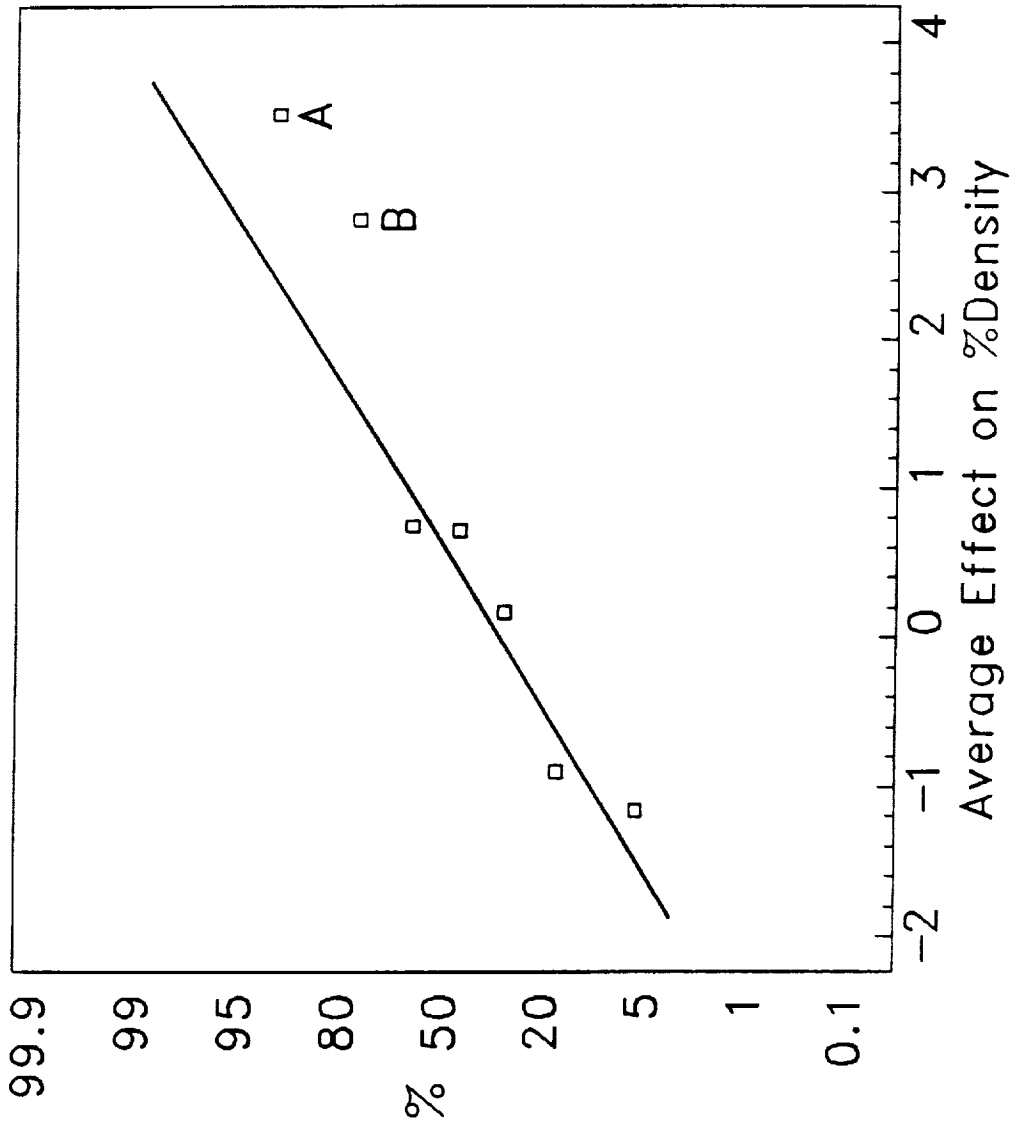
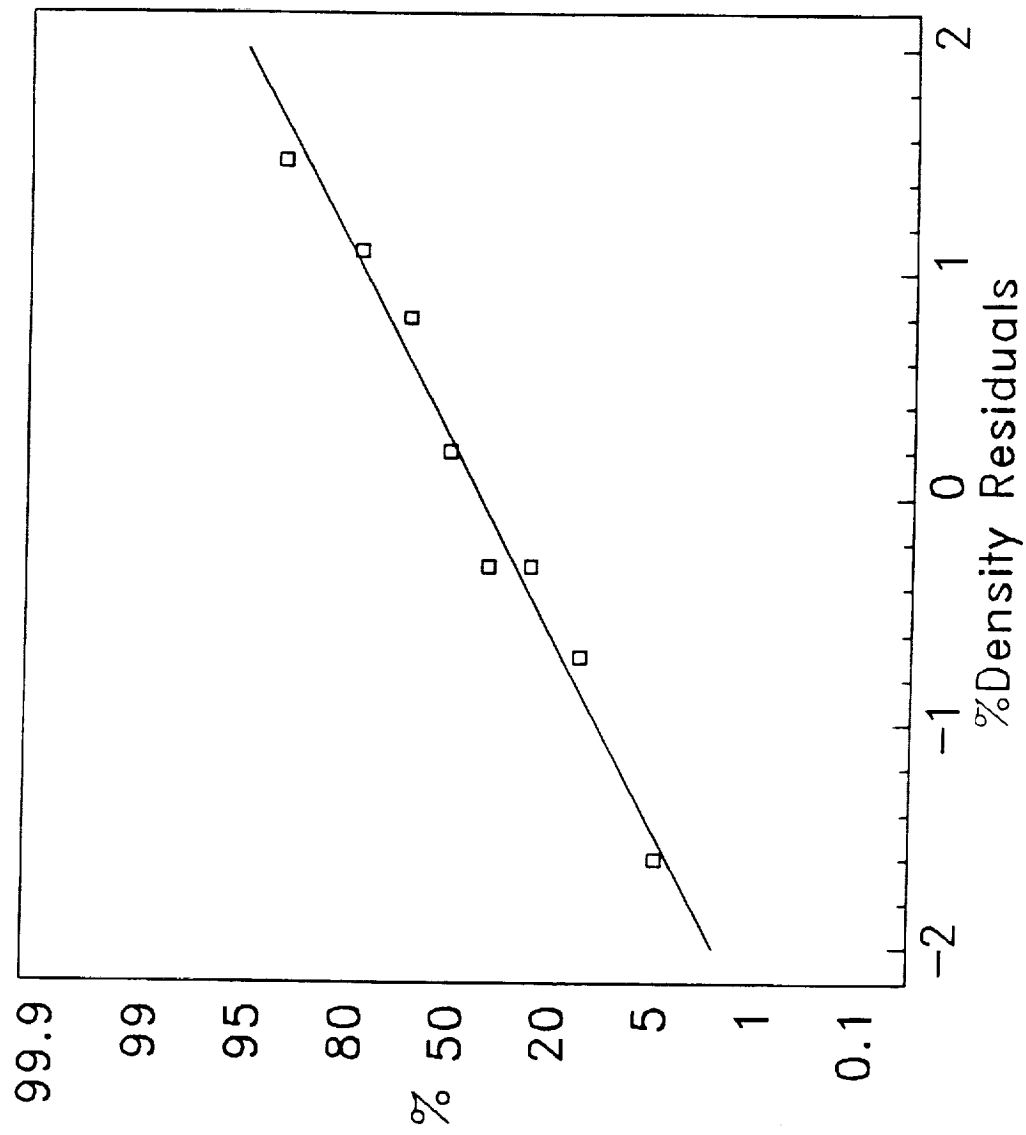


FIGURE 3

Task II / Matrix 2 Normal Probability Plot of Residuals



where Y = density of machined bars in g/cm³

X1 = % carbon

X2 = % boron

Figures 5 and 6 are plots of the observed data and the fitted model. Figure 5 is a three dimensional plot of the two models, one for the materials made with carbon black and the other for the materials made with resin as the source of carbon. In both models high density is favored primarily by high carbon contents, and to a lesser extent by low boron contents. Figure 6 shows two dimensional contour plots of the two models. These regression models are useful in planning further research to control density by compositional variation.

1.1.5 Experimental Design (Strength)

The design chosen was a 2⁵⁻¹ (five factors in 16 runs) of resolution V which provides no confounding between main effects and two-factor interactions, nor does it confound two-factor interactions with each other. It does confound two-factor interactions with three-factor interactions, but this was judged not to be a problem in this study. The confounding pattern can be found on page 382 of reference 4. Tables VII, VIII and IX show details of the design and values of the factors.

A second design was chosen after it became apparent that one of the factors (carbon source) gave particularly poor strength results at the higher level (carbon added as resin). Half of the data which involved the carbon source at the lower level (carbon added as carbon black) was then treated as a 2⁴⁻¹ design (four factors in 8 runs) of resolution IV. Resolution IV designs do not confound the main effects with two-factor interactions, but do confound two-factor interactions with each other.

Each of the experimental runs was performed with an average of 29 replicates. Although each bar was not carried through an individual dewaxing, sintering, annealing or HIP process, it was previously ascertained that these processes were under statistical process control and they did not add significantly to the strength variance. The entire set of 464 bars were randomized and processed in three dewaxing processes, eight sintering runs and six annealing runs. C. Daniel (Reference 5) discusses replication and randomization in some detail with some humor.

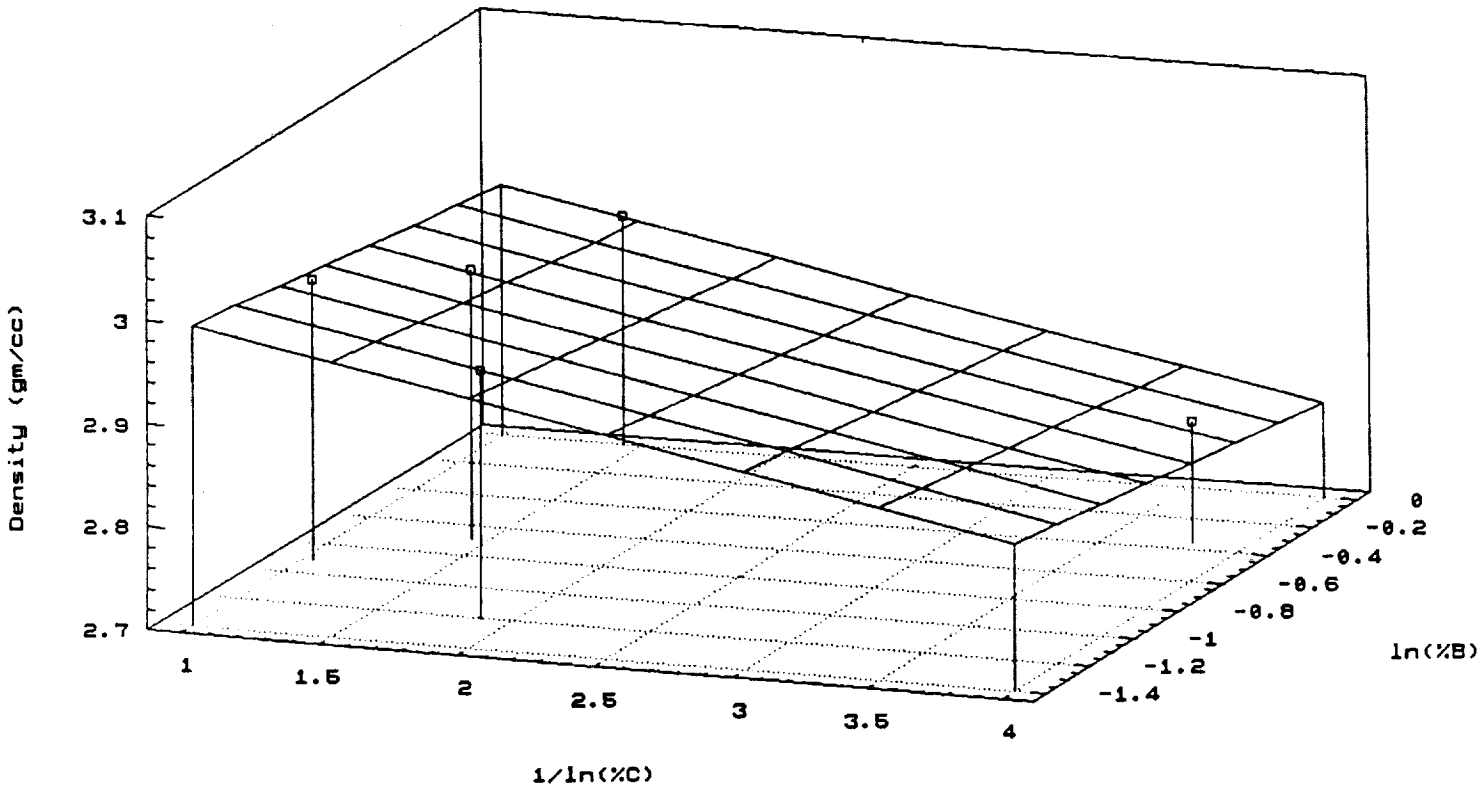
1.1.6 Factorial Analysis (Strength)

The results of the 5 factor - 16 run experiment is summarized in Table X and the effects, listed as the mean value of approximately 29 replicates, are listed in the Table.

5 Factors - 16 Runs Experiment

At least three effects, carbon source, and two, two-factor interactions appear significant, and these are boxed in Table X. Figure 7 is a plot of the normal probability against the mean value for strength and one sees clearly that the carbon source and the AC interaction (ratio and carbon

Figure 5
Observed Data & Fitted Model
Carbon Black Materials



Observed Data & Fitted Model
Resin Materials

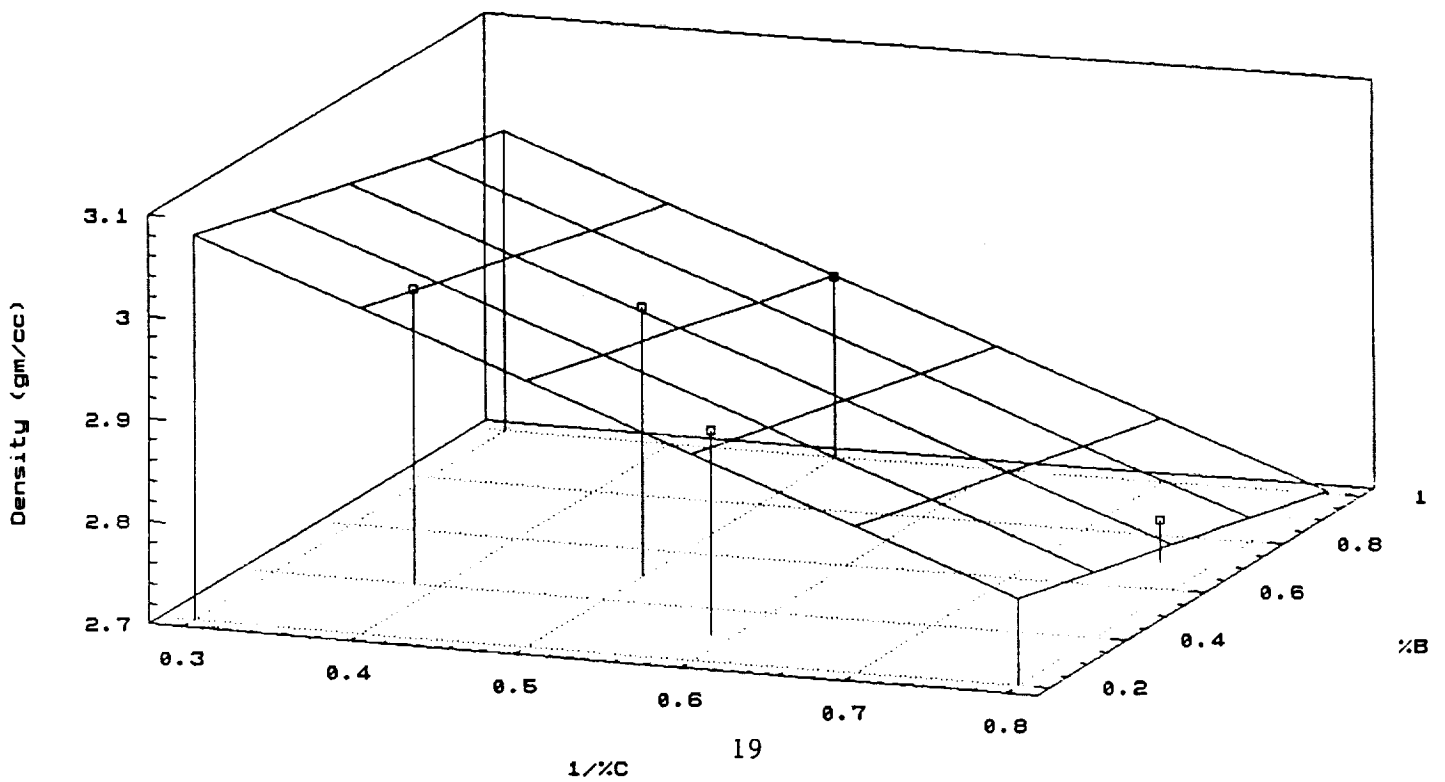
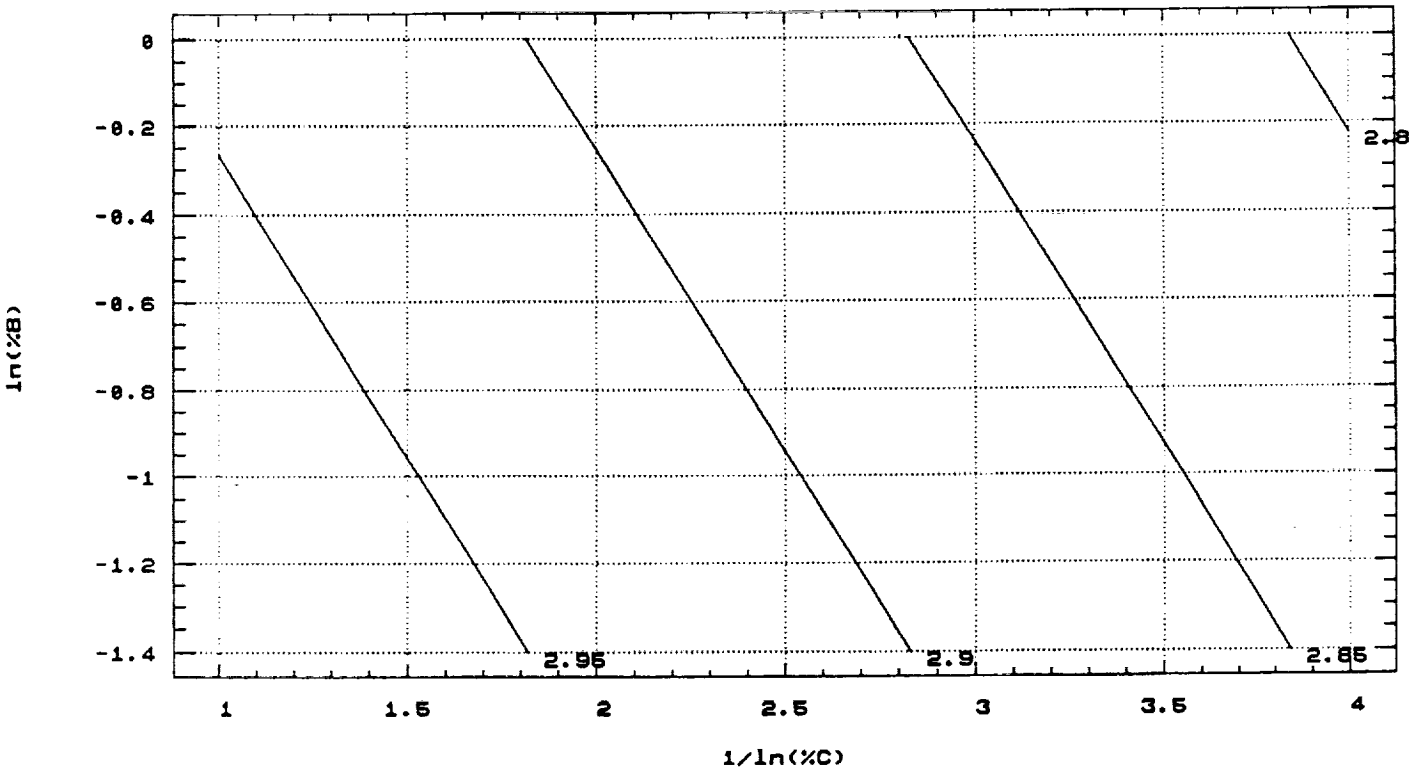


Figure 6
2D Contour Plot
Carbon Black Materials



2D Contour Plot
Resin Materials

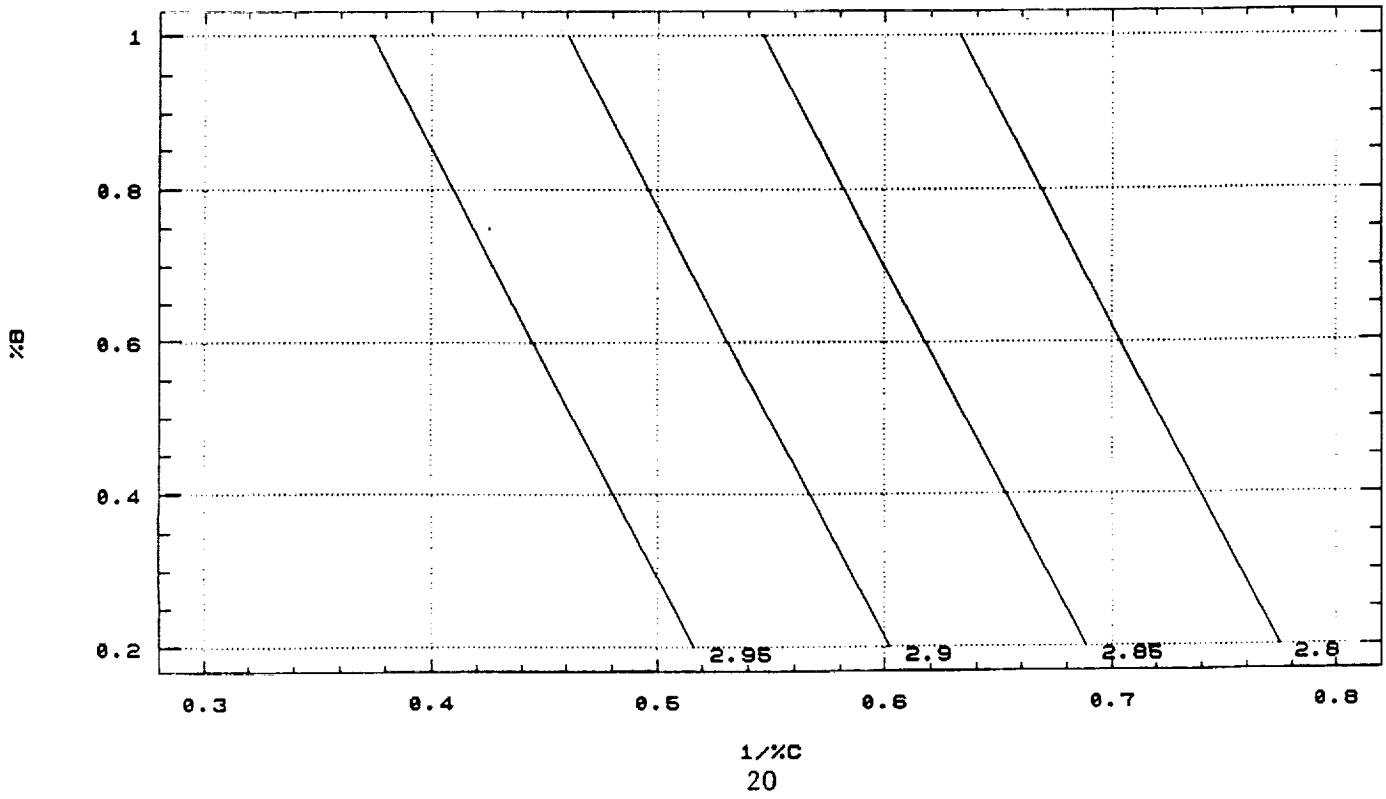


Table VII
2⁵⁻¹ Fractional Factorial Design

<u>Exp.#</u>	<u>A</u>	<u>B</u>	<u>C</u>	<u>D</u>	<u>E</u>
1	-	-	-	-	+
2	+	-	-	-	-
3	-	+	-	-	-
4	+	+	-	-	+
5	-	-	+	-	-
6	+	-	+	-	+
7	-	+	+	-	+
8	+	+	+	-	-
9	-	-	-	+	-
10	+	-	-	+	+
11	-	+	-	+	+
12	+	+	-	+	-
13	-	-	+	+	+
14	+	-	+	+	-
15	-	+	+	+	-
16	+	+	+	+	+

Table VIII
Task II/Matrix 2 Factors & Levels

<u>Factor</u>	<u>Name</u>	<u>-</u>	<u>+</u>
A	Carbon:Boron Ratio	2:1	6:1
B	Total %Additives	2	3
C	Carbon Source	C.Black	Resin
D	Anneal	No	Yes
E	HIP	No	Yes

Table IX
Task II/Matrix 2 Material Compositions

<u>Ratio</u>	<u>Total%</u>	<u>%Carbon</u>	<u>%Boron</u>
2:1	2	1.3	.7
6:1	2	1.7	.3
2:1	3	2.0	1.0
6:1	3	2.6	.4

TABLE X

TASK II/MATRIX 2 STRENGTH RESULTS

<u>EXP.#</u>	<u>C.SOURCE</u>	<u>MOR (KSI)</u>	<u>EFFECTS</u>	
1	C-BLACK	51.6	avg	49.69
2	C-BLACK	52.2	A	0.43
3	C-BLACK	48.9	B	2.00
4	C-BLACK	62.1	AB	-1.40
5	RESIN	41.8	C	-12.40
6	RESIN	41.8	AC	-9.04
7	RESIN	52.0	BC	-0.87
8	RESIN	36.8	DE	-4.16
9	C-BLACK	50.7	D	2.58
10	C-BLACK	63.4	AD	0.76
11	C-BLACK	53.5	BD	-1.13
12	C-BLACK	64.8	CE	-0.71
13	RESIN	47.1	CD	-1.83
14	RESIN	41.0	BE	-1.76
15	RESIN	50.2	AE	-0.39
16	RESIN	37.1	E	2.78

n = 27 - 30 samples

Normal Probability Plot of Effects
Mean Values

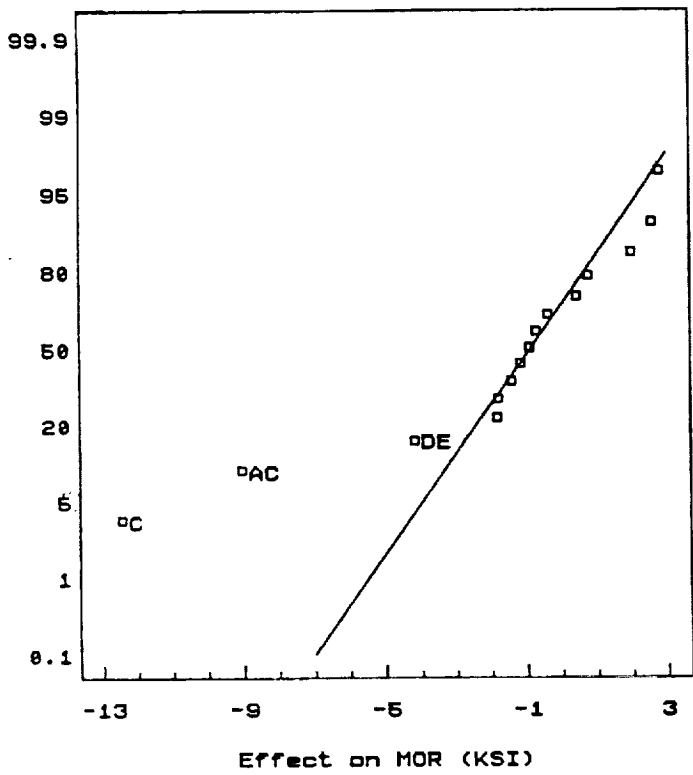


Figure 7

Factor C (Carbon Source)
Effect on MOR (KSI)

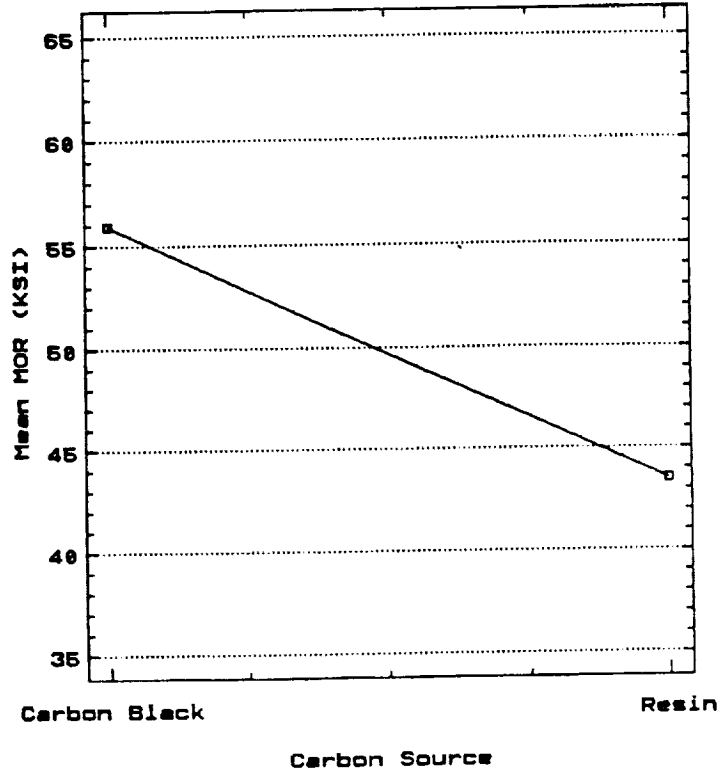


Figure 8

AC Interaction (Ratio & Carbon Source)
Effect on MOR (KSI)

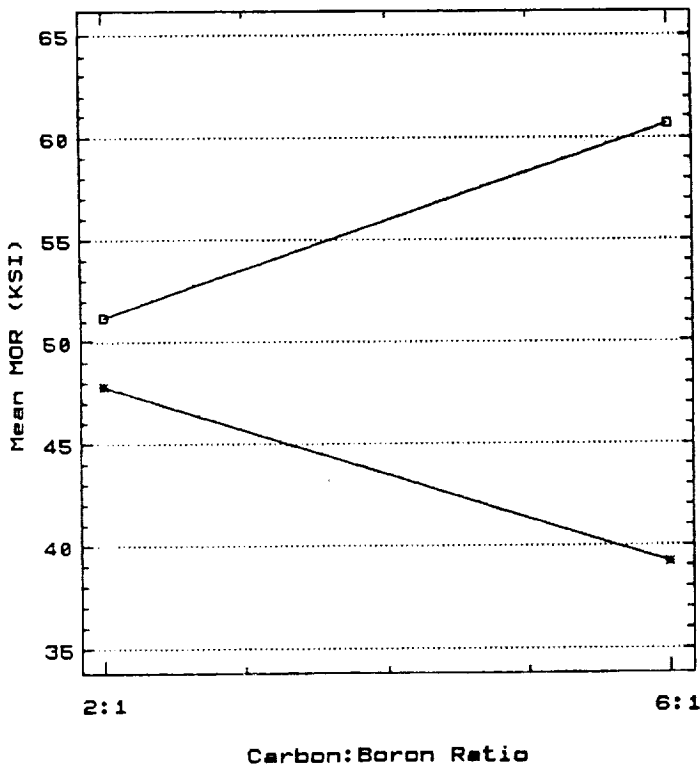


Figure 9

DE Interaction (Anneal & HIP)
Effect on MOR (KSI)

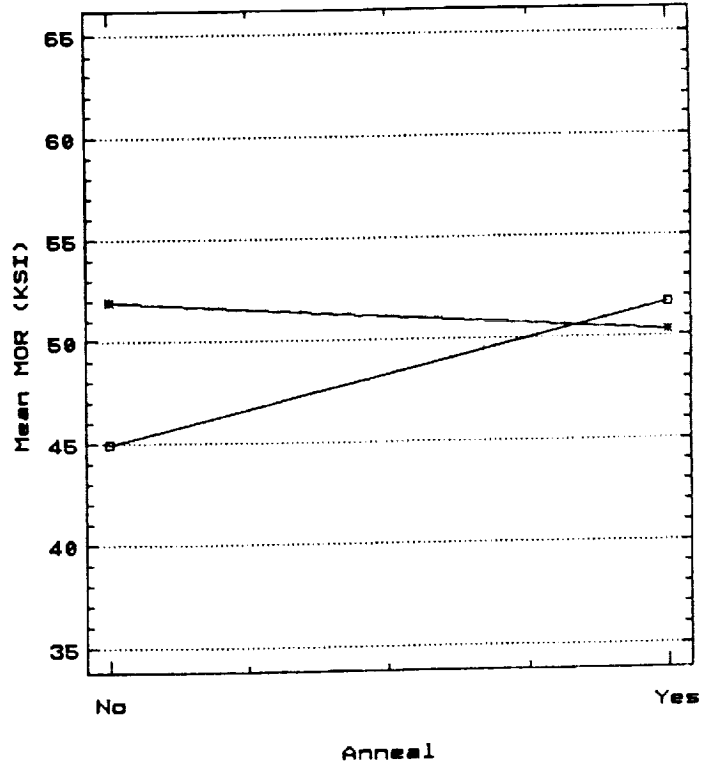


Figure 10

source) and possibly the DE interaction (anneal and HIP) are very strong effects. The carbon source effect and the interactions are plotted in Figures 8, 9 and 10.

For each run there are on average 29 replicates. To make use of this information the standard error of the effects was estimated with equation 1 (Reference 4):

$$V(\text{effect}) = 4 \frac{\sigma^2}{N} \quad \text{where } \sigma^2 \text{ is the variance and } N = 232$$

Table XI contains a listing of the 16 runs with the respective standard deviations and variance. A plot of the normal probability against the individual MOR strengths in Figure 11 shows that the strength data for a typical set of replicates are normally distributed. Calculations lead to a value of 0.74 for the $V(\text{effect})$ and 0.86 for the estimated standard error. The scaled t distribution shown in Figure 12 also indicates that not only are the carbon source and the 2 two-factor interactions significant, but the D effect (anneal) and E effect (HIP) are also significant.

An examination of the data and effects show that the C factor (carbon source) is very strong and that carbon introduced as carbon black resulted in much stronger material than the material containing the carbon from resin. Since the goal of the program is to improve the strength of silicon carbide, it was desirable to further investigate the 8 runs in which carbon black was the source of carbon.

4 Factors - 8 Runs Analysis

Table XII lists the design of the 4 factor - 8 run experiment and shows the mean MOR strength as the yield of the experiment and the calculated effects. A normal probability plot of the effects is shown in Figure 13. From the plot in Figure 13 one sees that the factor A (ratio C:B) appears to be important, but there are not enough data to draw conclusions as to the significance of factors D (HIP) and C (anneal).

Again making use of the 29 replicates for each run, we have calculated the variance of the effects with the use of equation 1, given above, and find that the $V(\text{effect})$ is 0.96 and the estimated standard error is 0.98. In Figure 14 is shown the scaled t distribution and the dot plot of the effects and it is seen that all four factors, A (ratio C:B), B (total %), C (anneal), and D (HIP) are significant. A normal probability plot of residuals with these four factors is shown in Figure 15 which tends to support these conclusions, since the residual plot appears to be linear.

Microstructure

As the strength of the materials improves, the difficulty in finding the fracture origins increases. A few of the weaker fractured MOR bars could be observed in the scanning electron microscope and Figure 16 is an example. This sample is from Batch 4, experiment 12 and has carbon added as carbon black, a 6:1 ratio of carbon to boron, and 3% total additives. It had a low strength of 320 MPa (46.5 Ksi) and one can see the sub-surface failure initiation site in the Figure 16(a). Higher magnification

TABLE XI

TASK II/MATRIX 2 STANDARD DEVIATION
AND VARIANCE OF REPLICATES

<u>EXPT.NO.</u>	<u>MEAN.MOR</u>	<u>STD.DEV</u>	<u>VARIANCE</u>	<u>NUMBER SAMPLES</u>
1	51.56	7.88	62.09	30
2	52.24	8.25	68.06	28
3	48.91	6.38	40.70	27
4	62.13	5.79	33.52	29
5	41.76	7.41	54.91	29
6	41.78	9.11	82.99	29
7	52.04	9.80	96.04	28
8	36.79	8.34	69.56	29
9	50.69	5.28	27.88	29
10	63.41	9.17	84.09	30
11	53.54	6.23	38.81	28
12	64.80	8.72	76.04	30
13	47.09	9.24	85.38	29
14	40.98	7.37	54.32	28
15	50.19	9.20	84.64	30
16	37.09	7.46	55.65	28

Normal Plot of Strength of a Typical
Group of Replicates

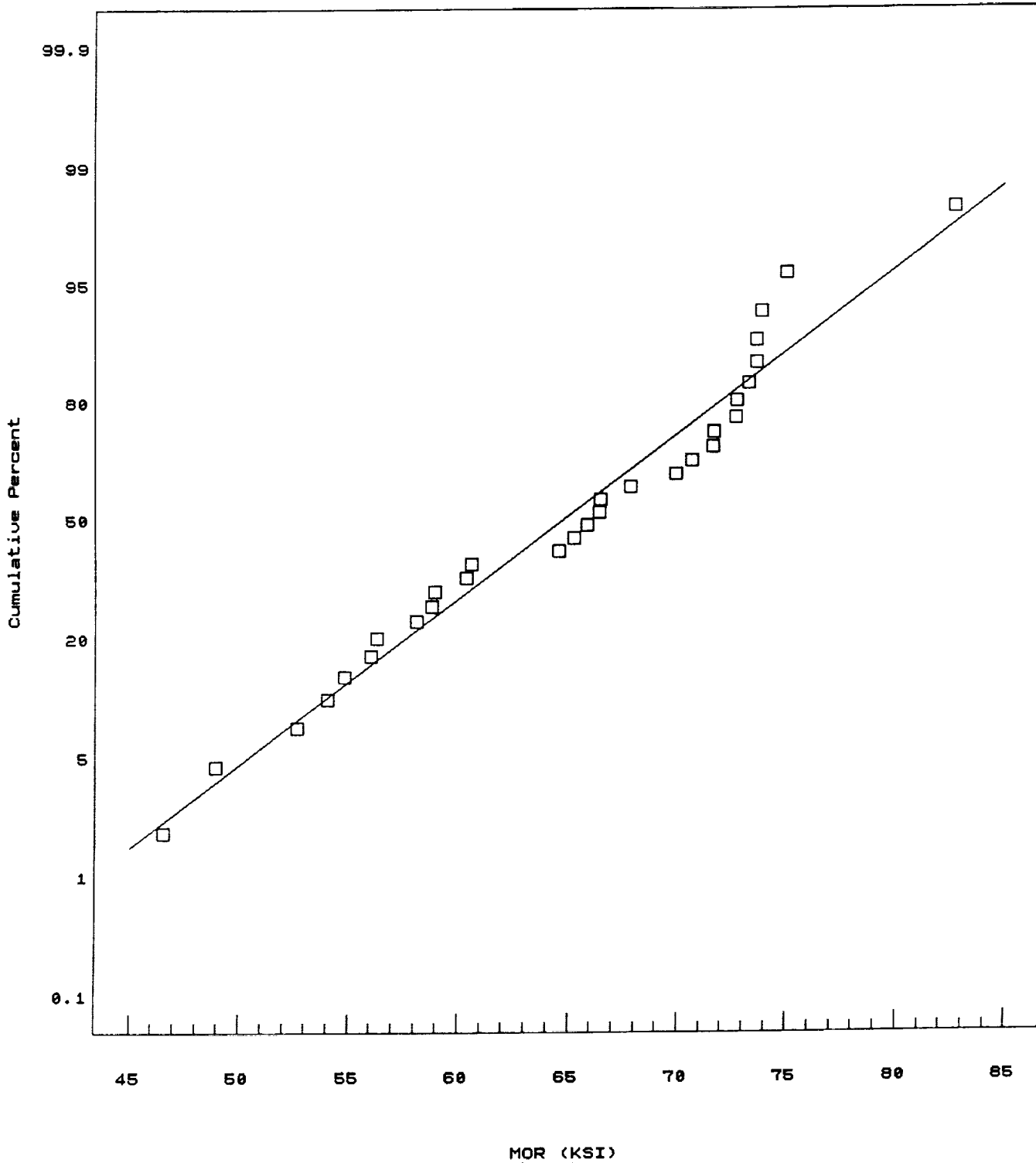


FIGURE 11

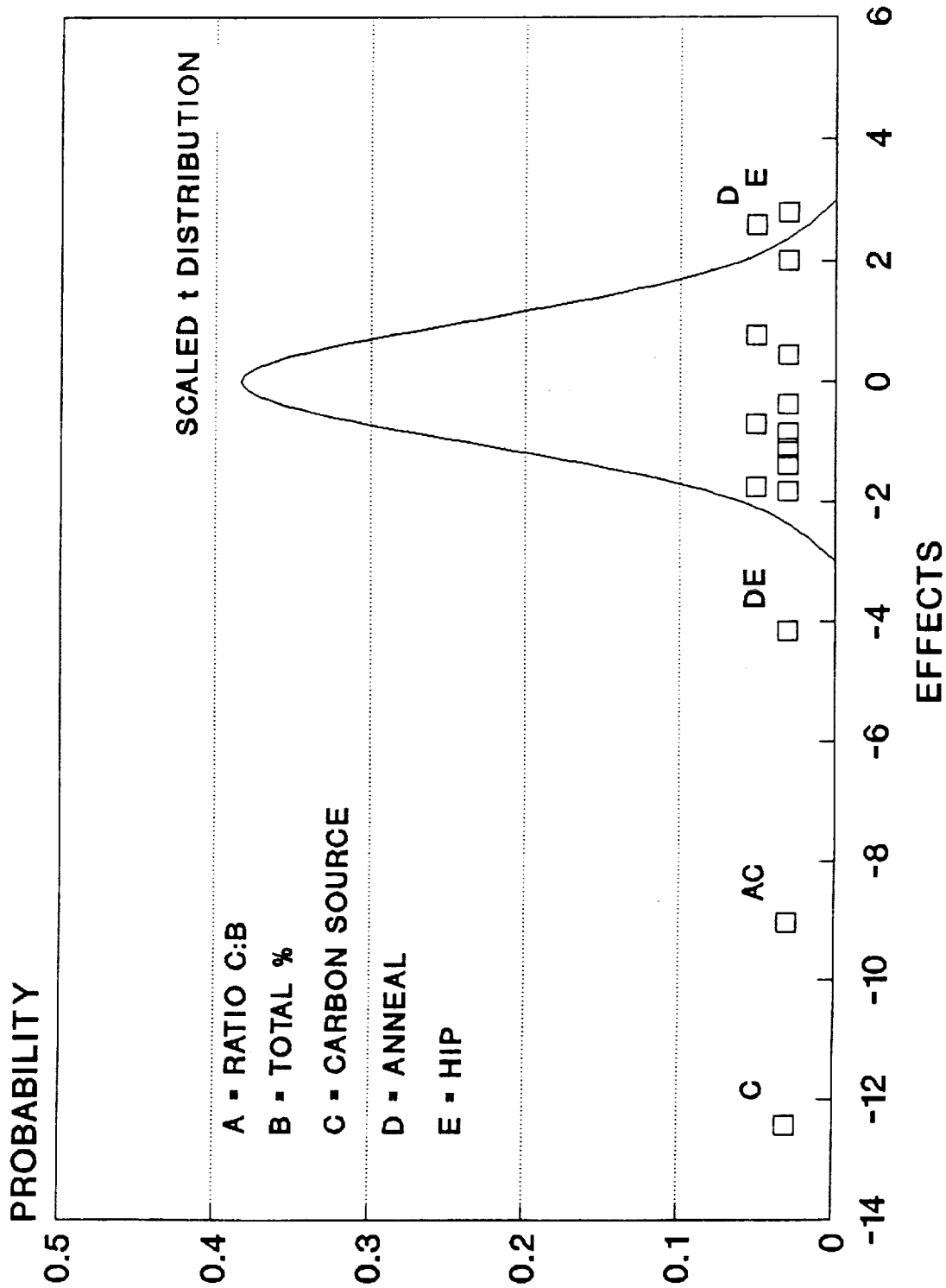


FIGURE 12

TABLE XII

TASK II/MATRIX 2

YIELDS AND EFFECTS IN 4-FACTOR, 8-RUN ANALYSIS

<u>YIELD MOR (KSI)*</u>	<u>EFFECTS (KSI)</u>	<u>DESIGNATION</u>
51.56	55.91	AVERAGE
52.24	9.47 +/- 1.0**	RATIO C:B
48.91	2.87	TOTAL % C+B
62.13	2.77	INTERACTION
50.69	4.40	ANNEAL
63.41	2.52	INTERACTION
53.54	-0.75	INTERACTION
64.80	3.50	HIP

* Mean strength of approximately
30 samples

** Estimated standard error

Normal Plot of Effects for 4-Factor

8-Run Analysis

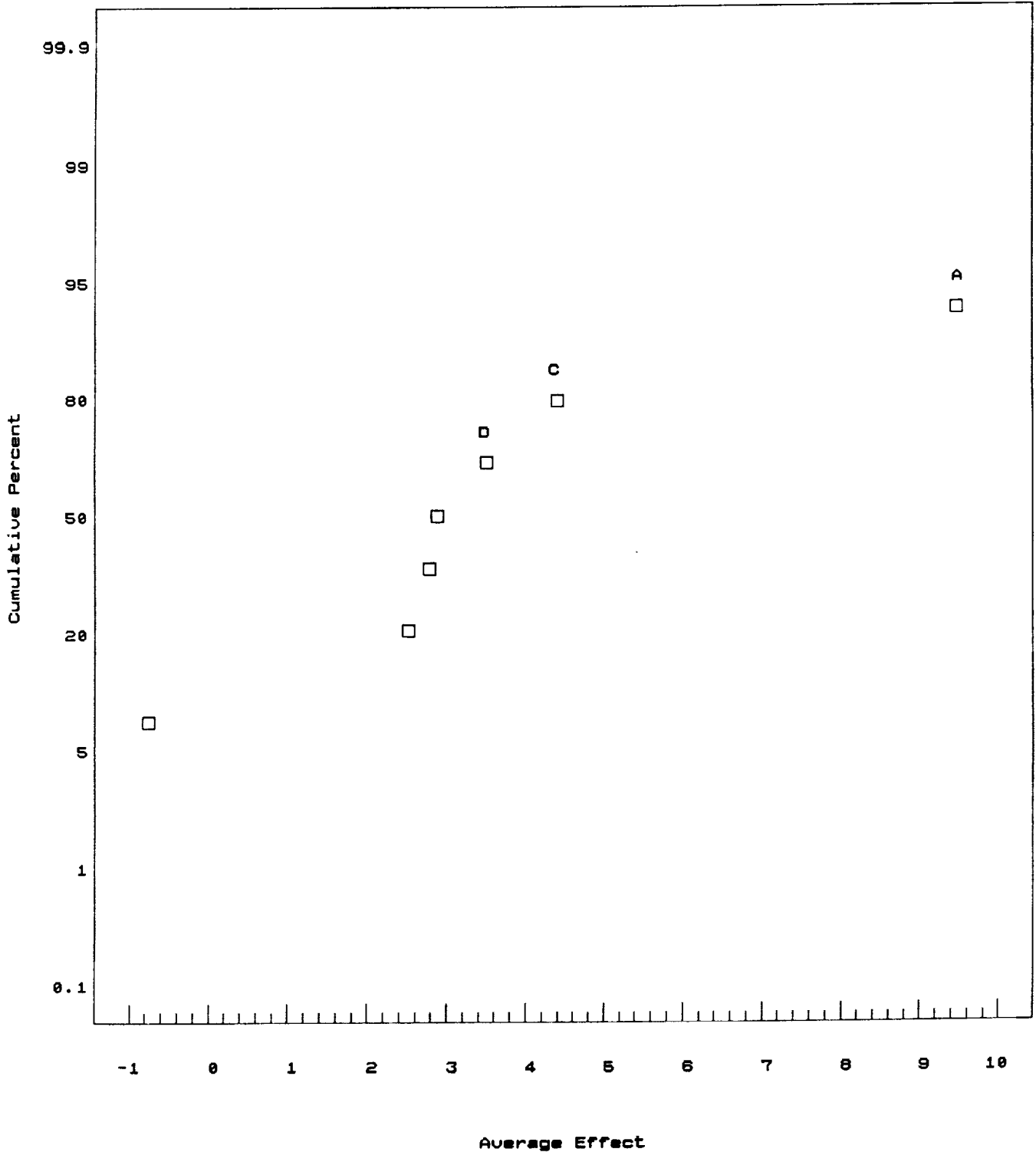


FIGURE 13

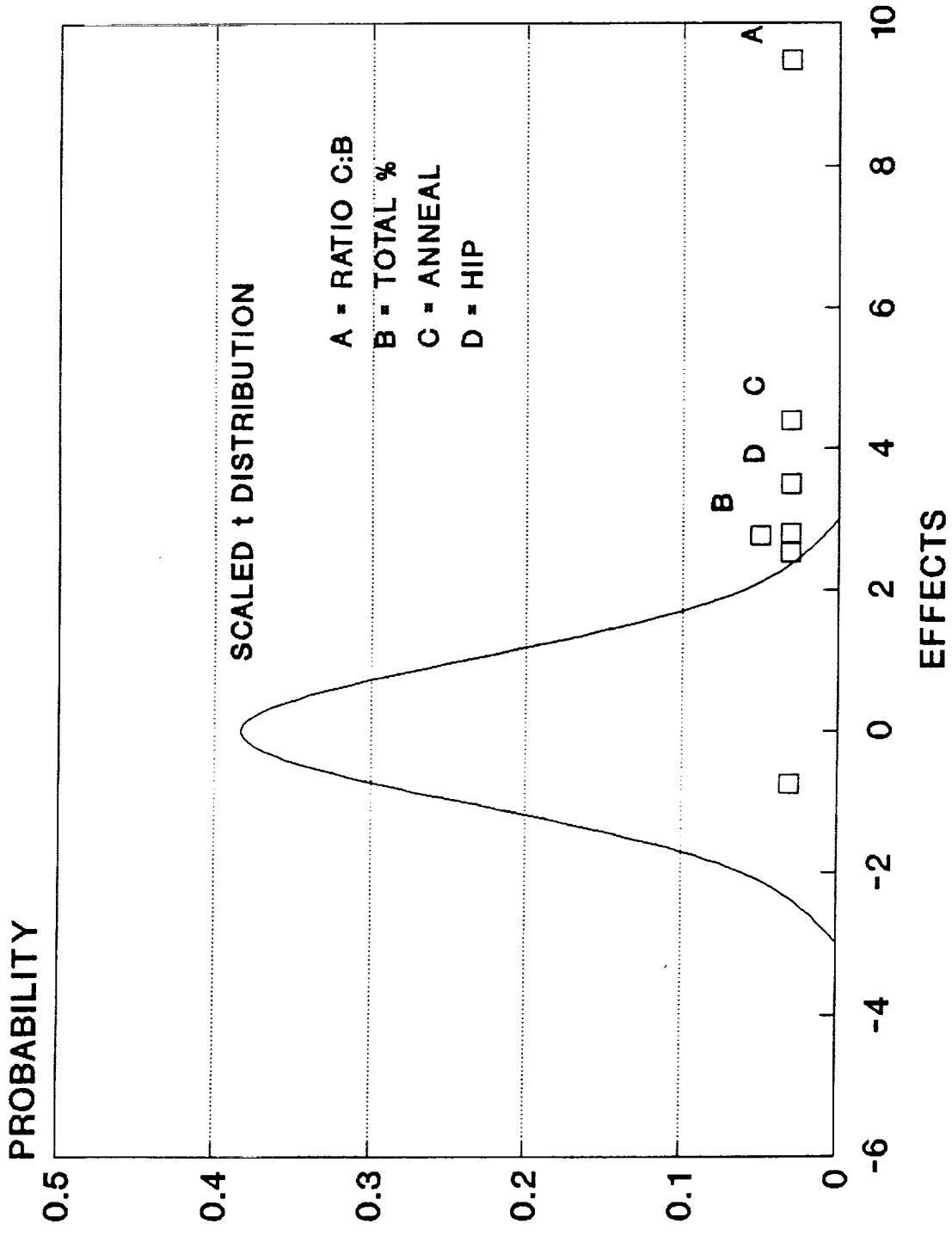


FIGURE 14

Task II / Matrix 2 Normal Probability Plot of Residuals

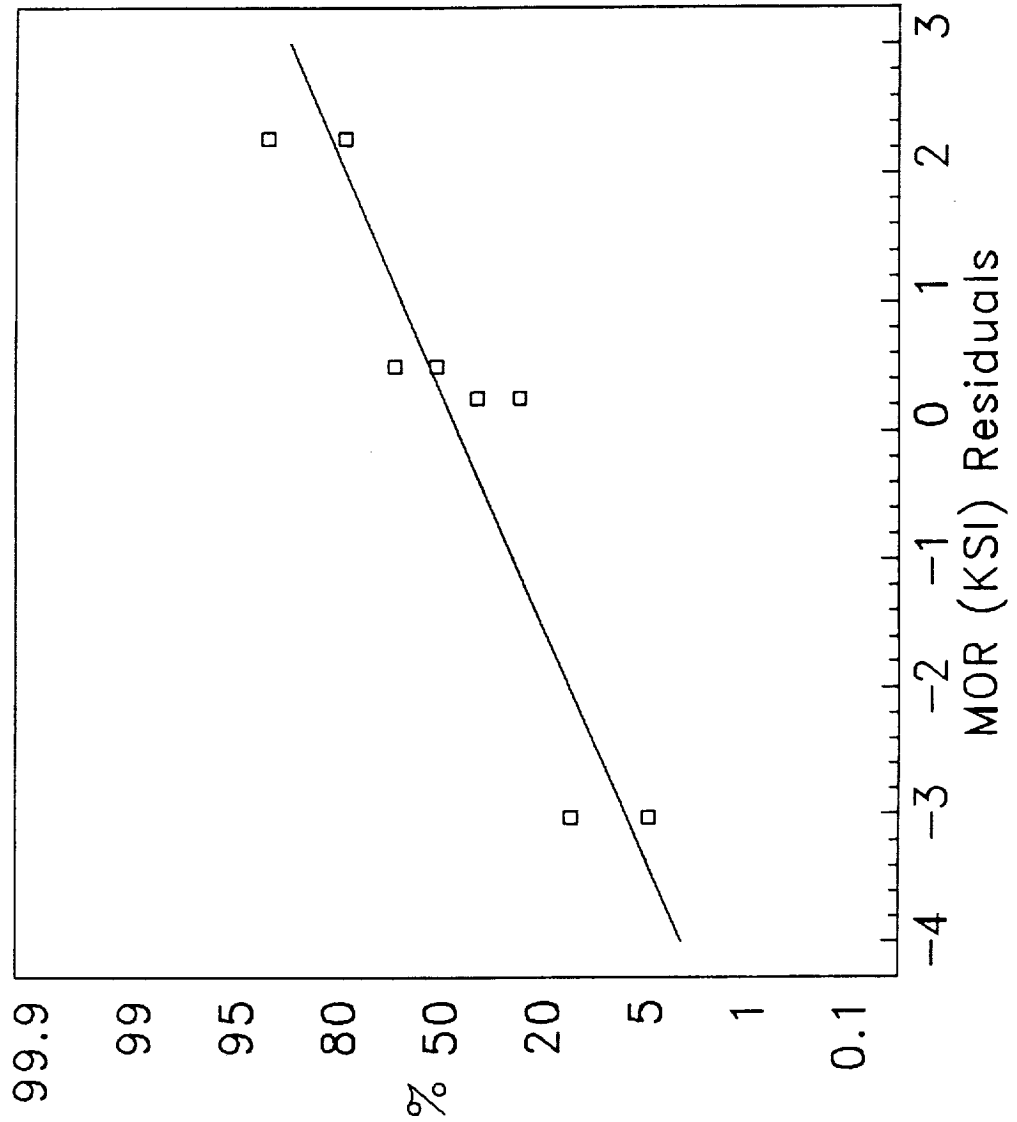


FIGURE 15

ORIGINAL PAGE
BLACK AND WHITE PHOTOGRAPH

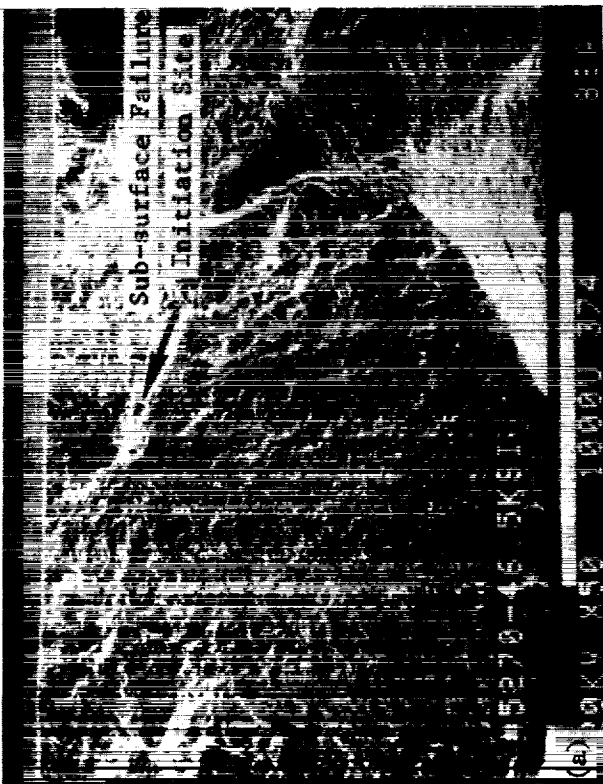
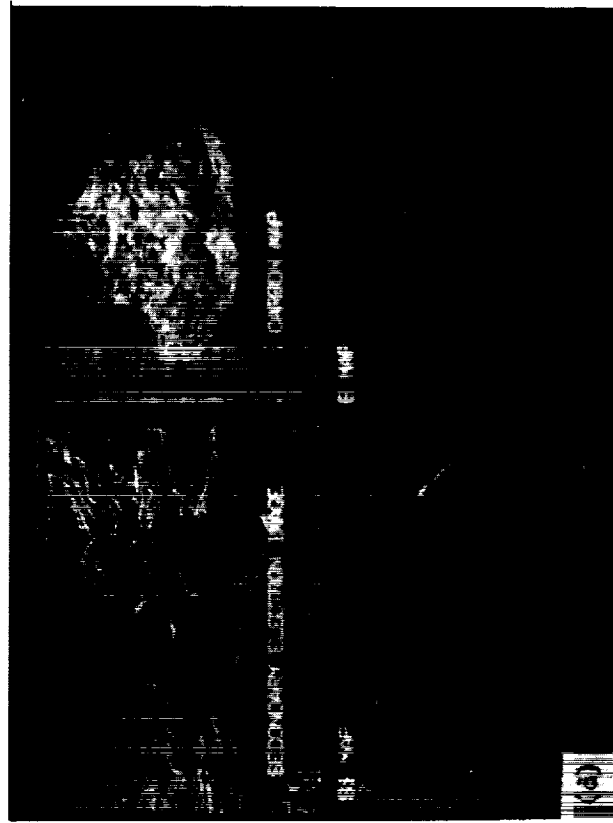
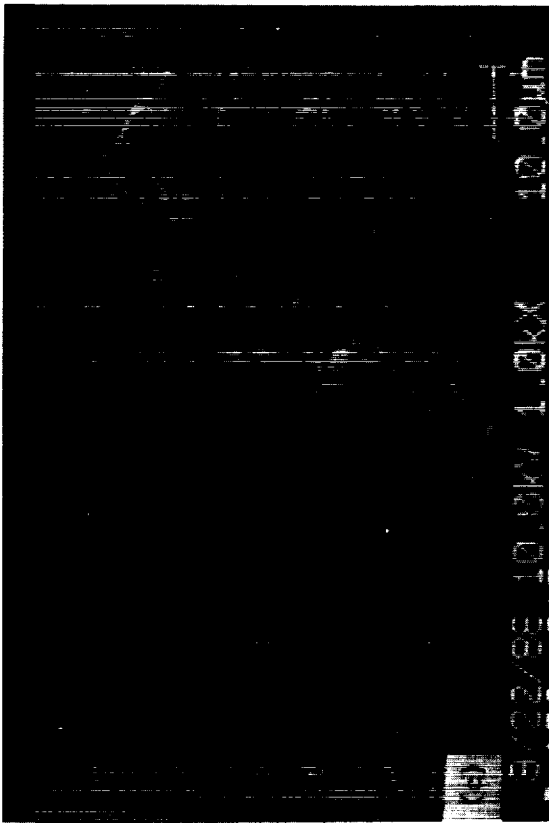


FIGURE 16

is shown in sections b and c of the figure and a secondary electron image analysis is seen in section c. The conclusion is that this flaw is a carbon agglomerate of about 100 micrometers in diameter with no silicon or boron present. Such a flaw may be introduced into the material as a carbon agglomerate which was not dispersed by the mixing process, or it may be an air-borne carbon particle introduced in the processing environment.

1.1.7 Conclusions (Strength)

From this experiment, to produce higher strength silicon carbide, the following conclusions are drawn:

1. Carbon added as carbon black is significantly better than carbon added as resin, which may be a result of the more uniform distribution with carbon black since resin was observed to agglomerate during the drying process.
2. A C:B ratio of 6:1 is significantly better than a ratio of 2:1, when the carbon source is carbon black. This may be a function of the oxygen content of the starting powders since carbon reacts with the oxygen during the sintering process.
3. The total % additives (boron + carbon) of 3% is better than 2%. Again, the oxygen content of the starting powders may influence this result.
4. Annealing significantly improves strength. This result may be due to the blunting of surface flaws by the creation of a silica coating.
5. The HIP process significantly improves strength. This effect can be considered as a result of the improved density leading to a reduction in flaw or porous region size.

1.1.8 Recommendations for Future Work (Strength)

Improvements in strength within the present Ford process can probably be made by optimizing the carbon:boron ratio and the total amount of additives. It is recommended that a three-level or four-level factorial experiment (Reference 6) be performed with these two factors (C:B ratio and total additives) in order to investigate the response surface close to the improved values determined from this two-factor experiment.

2. TASK VII MATERIAL AND PROCESS IMPROVEMENT

2.1 Characterization of SiC Polytypes by Nuclear Magnetic Resonance

The chemical compound, silicon carbide, exists in many crystalline modifications which can be grouped in either an hexagonal alpha-SiC which has the wurtzite-type ZnS structure, or a cubic beta-SiC which has a diamond structure. The structural complexity is a result of the numerous stacking sequences in the crystal. High-resolution solid-state nuclear magnetic resonance spectroscopy has been reported which appears to be highly sensitive to the lattice structure details (Ref. 7). Figure 17 shows the three types of silicon first and second neighbor environments reported in SiC polytypes. Only Type A environment is found in cubic (beta) crystals. The 6H hexagonal form contains equal numbers of Types A, B and C environments. Other polytypes contain Types A, B and C in different ratios, which may be distinguishable by magic angle spinning nuclear magnetic resonance.

The two sources of beta-SiC powder used in this program are Ibiden UF SiC, procured from Japan, and a beta-SiC powder from the Superior Graphite Company, Chicago, Illinois. The magic angle spinning, nuclear magnetic resonance spectra (m.a.s. n.m.r.) were obtained at the Ford Scientific Laboratory by Dr. Keith Carduner for these two powders, along with spectra of other SiC powders which were available in the laboratory. Figures 18 and 19 show the spectra of the Ibiden and the Superior Graphite powders, respectively. Figure 20 contains the spectra of an alpha-SiC powder from the Starck Chemical Company in Germany, and the spectra of a beta-SiC powder also from Starck is shown in Figure 21. The spectra for the alpha powder is characteristic of the spectra reported to be the 6H hexagonal polytype (from X-ray data) in the above reference. Figure 21 shows a very sharp peak for the beta-SiC from Starck, which is narrower than the peak observed from the Ibiden beta-SiC powder. These results appear to be consistent with the above referenced study. The difference in the sharpness of the m.a.s. n.m.r. spectra for the Ibiden and Superior Graphite powders in comparison to the Starck beta powders suggests that the Ibiden and Superior Graphite powders are formed under similar conditions and the Starck powder is formed under somewhat different conditions. Closer inspection of all these spectra indicates that they form a rather unique fingerprint for each of the powders.

Another beta SiC powder, provided by Alcoa, is shown in Figure 22 and one sees a very sharp, single peak indicative of pure beta (cubic) SiC. The spectra for the Alcoa powder is very similar to the spectra for the Starck beta powder and much sharper than the spectra derived from the Ibiden and Superior Graphite powders. The differences in the powder spectra are probably indicative of the different details such as the starting powders, temperature, time and environment, in the manufacturing processes for these powders.

N.M.R. spectra for a sintered sample of Attritor 1/annealed material were generated and is shown in Figures 23. The spectra is primarily that of an alpha SiC material, indicating that during the sintering process, and perhaps the annealing process, the beta SiC powder transformed from cubic SiC to the alpha polytypes of rhombohedral and hexagonal structures.

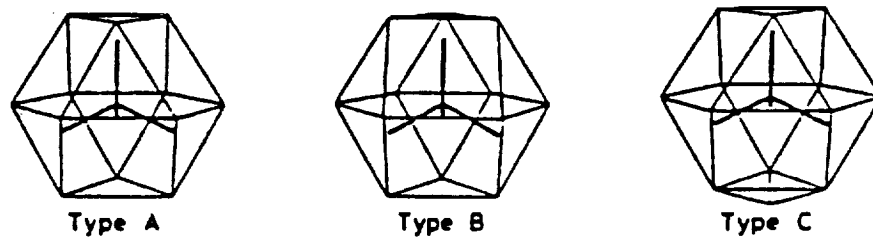


FIGURE 17 Three distinctive types of silicon atom environment found in SiC polytypes. (G. R. Findlay, J. S. Hartman, M. F. Richardson and B. L. Williams, *J. Chem. Soc., Chem. Comm.*, pp. 159 - 161, 1985).

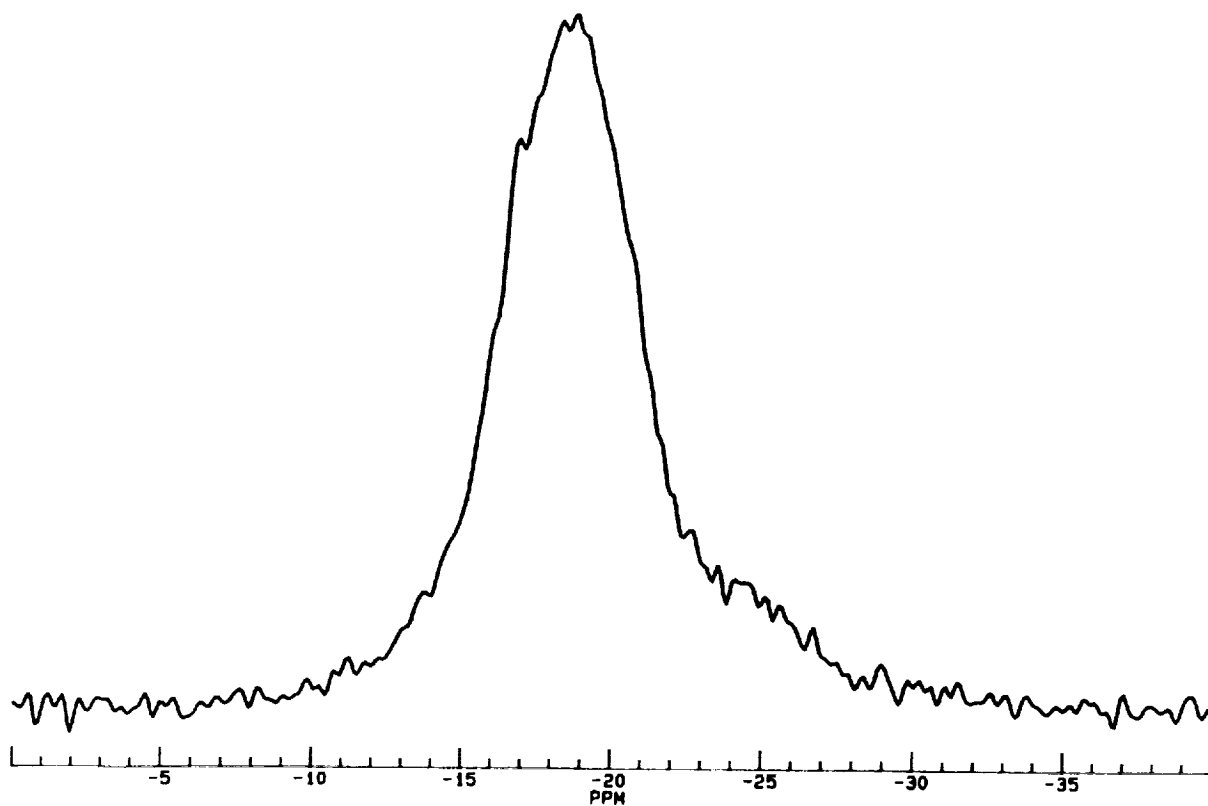


FIGURE 18 Magic angle spinning, N.M.R. spectra of Ibiden beta SiC.

SUPERIOR GRAPHITE - BETA-SiC

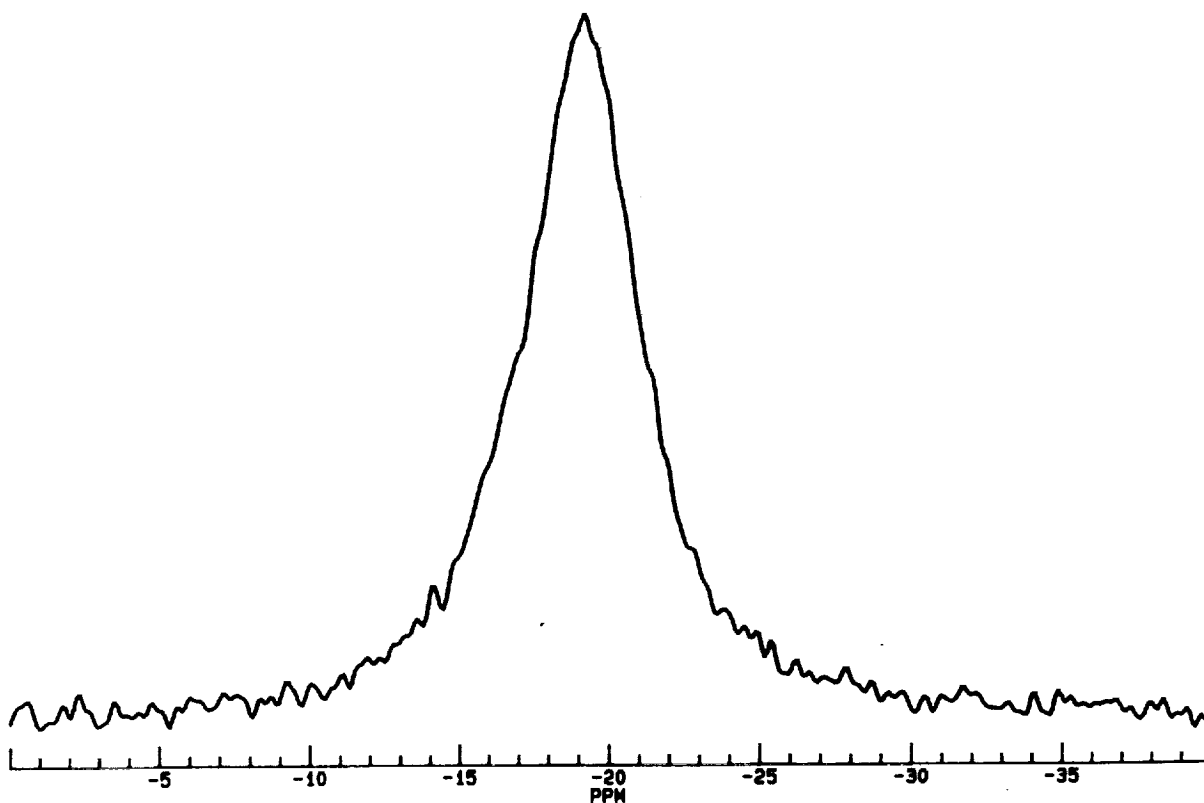


FIGURE 19 Magic angle spinning N. M. R. spectra of Superior Graphite beta SiC.

STARCK A1 - ALPHA-SiC

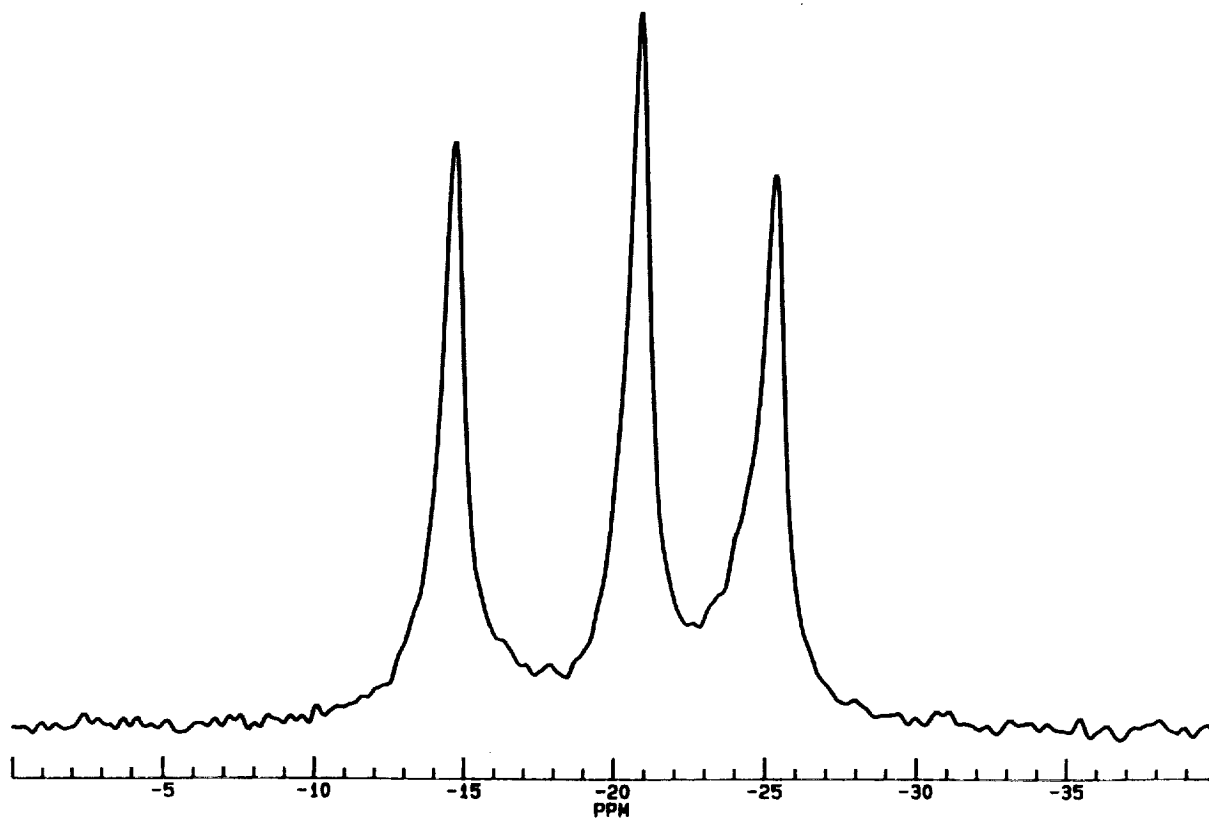


Figure 20 - Magic angle spinning, N. M. R. spectra of Starck alpha SiC.

STARCK B10 - BETA-SiC

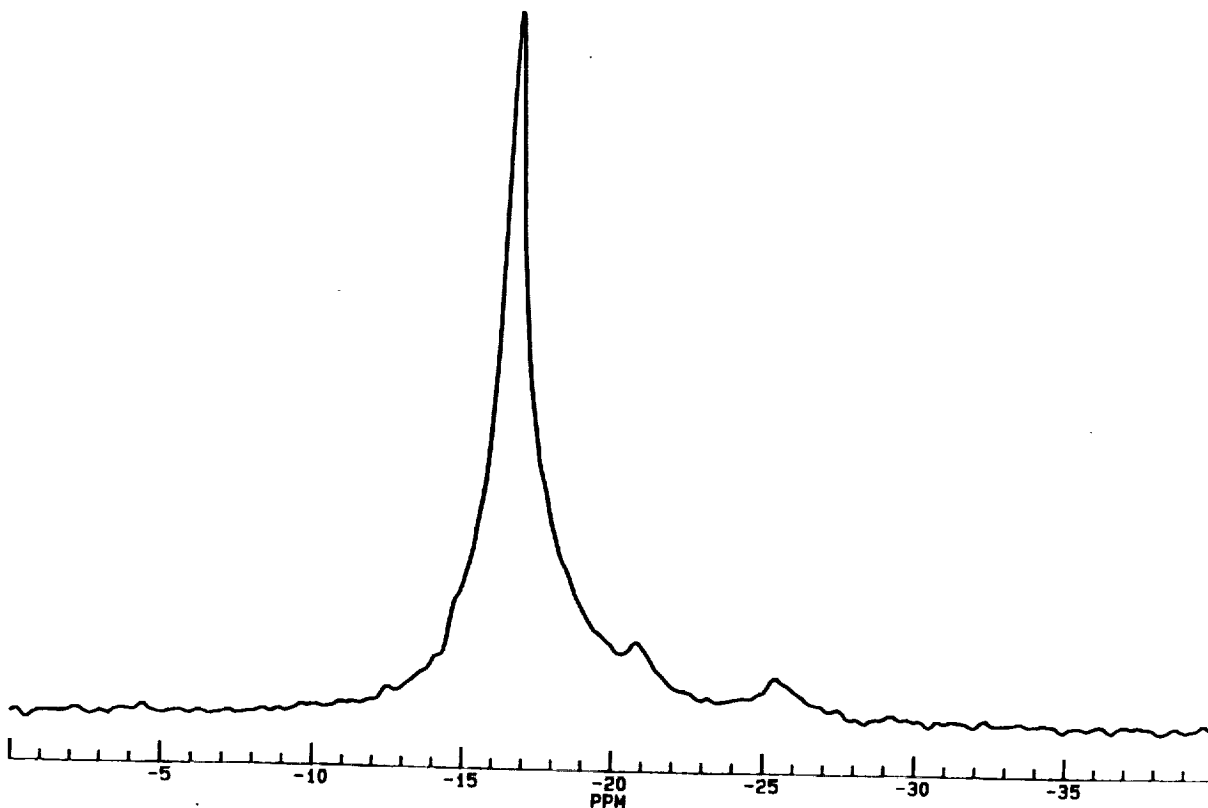


Figure 21 Magic angle spinning N. M. R. spectra of Starck beta SiC.

ALCOA BETA-SiC

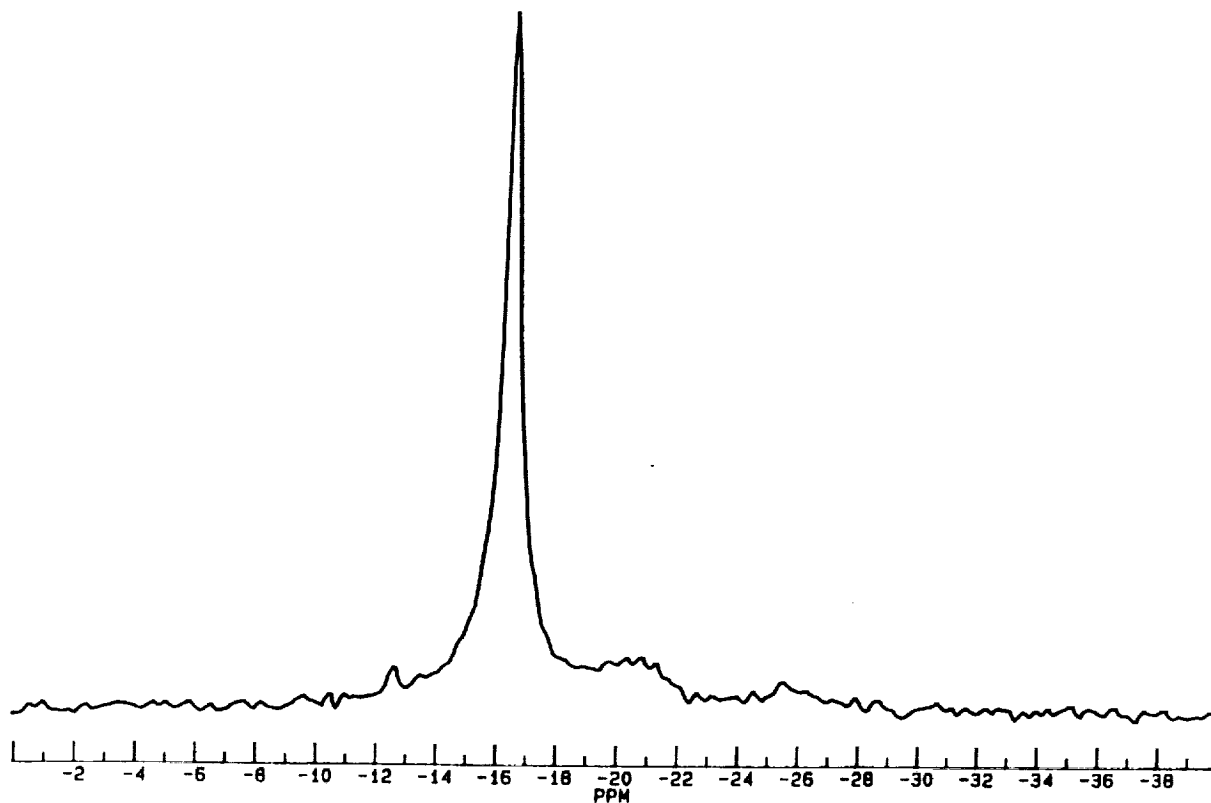


FIGURE 22

SAMPLE 4083B

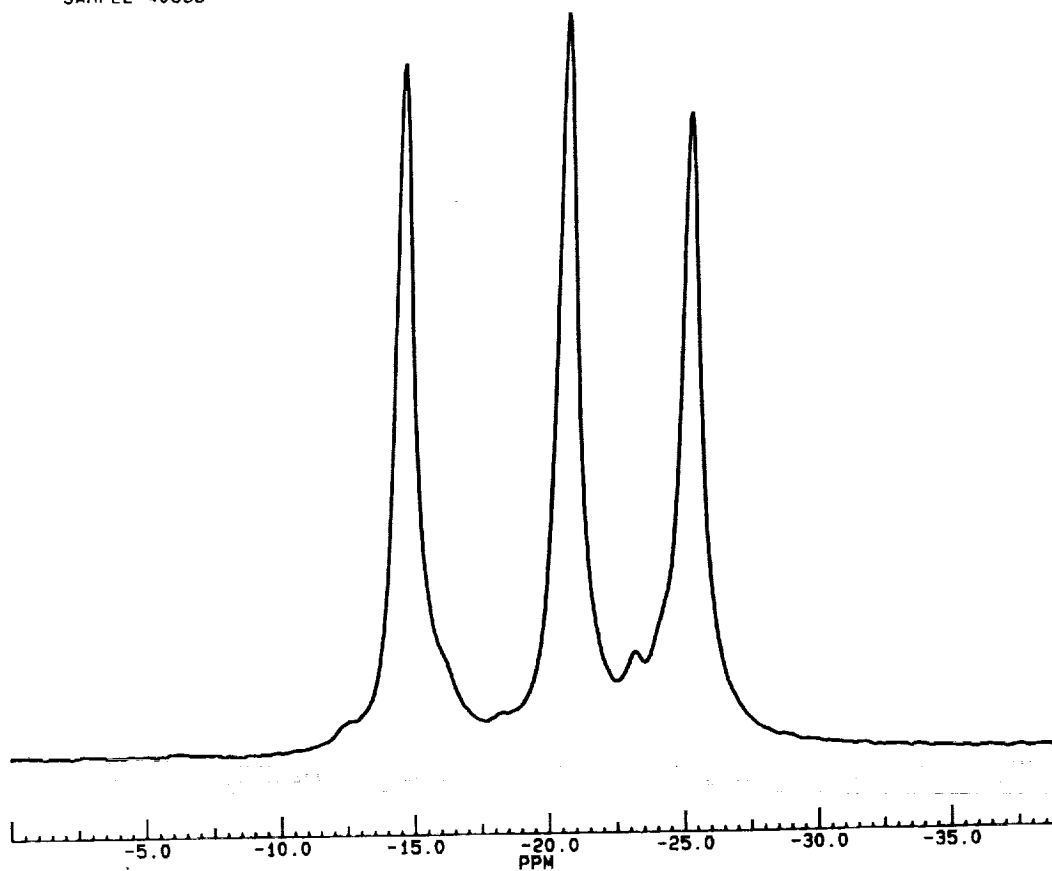


FIGURE 23

We conclude from this study that the powders and sintered samples can be rather uniquely characterized by the m.a.s. n.m.r. spectra, which may be useful in a statistical process control system for processing, and that the crystal environment can be determined and the crystal form implied from the spectra.

2.2 Task VII - Matrix 12 (Attritor Speed Optimization Study)

2.2.1 Sample Preparation

Although much information on composition and carbon source was derived from the Task II - Matrix 2 study, the strengths were disappointing since the highest mean strengths were only about 65 Ksi. Past results with attritor mixed samples prepared at the laboratory of the attritor manufacturer were considerably better with strengths greater than 80 Ksi (Ref. 3). Further investigation into the conditions of operation of the attritor mill indicated that the rotational speed strongly influences the degree of homogeneity of the mixes. A study of the effect of rotational speed of the attritor on the density and strength of the sintered SiC was begun to clarify these results. The study was focused on the density and strength of sintered and machined, and machined and annealed MOR bars as a function of attritor RPM during the mixing process. The time of the attritor mixing was held constant.

2.2.2 Analysis of Data and Discussion of Results

The mean MOR strengths are listed in Table XIII along with the number of samples in each group (n) and the standard deviation (s). The strong effect of attritor rotational speed is clearly seen from the data and this effect is plotted in Figure 24. Attempts to model the effect of attritor speed on density and strength yielded linear regression models of the following form for the speed range studied:

Density: $Y = 91.5 + 0.0156 X$ R^2 (adj.) = 93.2%
where Y = sintered density in % theoretical density
X = rotational speed of the attritor in revolutions per minute (rpm)

Machined MOR strength: $Y = 41.3 + 0.063 X$ R^2 (adj.) = 98.8%
where Y = strength in Ksi
X = rotational speed of the attritor in rpm

Machined-annealed MOR strength: $Y = 42.3 + 0.084 X$ R^2 (adj.) = 94.9%
where Y = strength in Ksi
X = rotational speed of the attritor in rpm

Further statistical tests indicated that the effects of attritor speed on both density and strength are highly significant.

The beneficial effect of the increasing rotational speed of the attritor on the density and strength of the sintered material is believed to be a result of the improved homogeneity of the fluid-mixed batches. Dip-slide samples taken during the attritor mixing process tend to show a rather

TABLE XIII

Properties of SiC as a Function
of Attritor Rotational Speed

	<u>Speed (RPM)</u>								
	<u>115</u>			<u>350</u>			<u>460</u>		
	<u>Strength (ksi)</u>								
	$\frac{n}{}$	$\frac{\bar{x}}{}$	$\frac{s}{}$	$\frac{n}{}$	$\frac{\bar{x}}{}$	$\frac{s}{}$	$\frac{n}{}$	$\frac{\bar{x}}{}$	$\frac{s}{}$
Machined	27	48.9	6.4	15	62.4	8.6	12	71.0	6.2
Machined + Annealed	10	51.1	8.4	10	74.4	9.7	14	79.1	10.8
	<u>Sintered Dentisy (% T. D.)</u>								
	30	93.5	0.4	48	96.4	0.2	61	99.1	0.1

Task VII/Matrix 12
Effect of Attritor RPM on MOR & Density

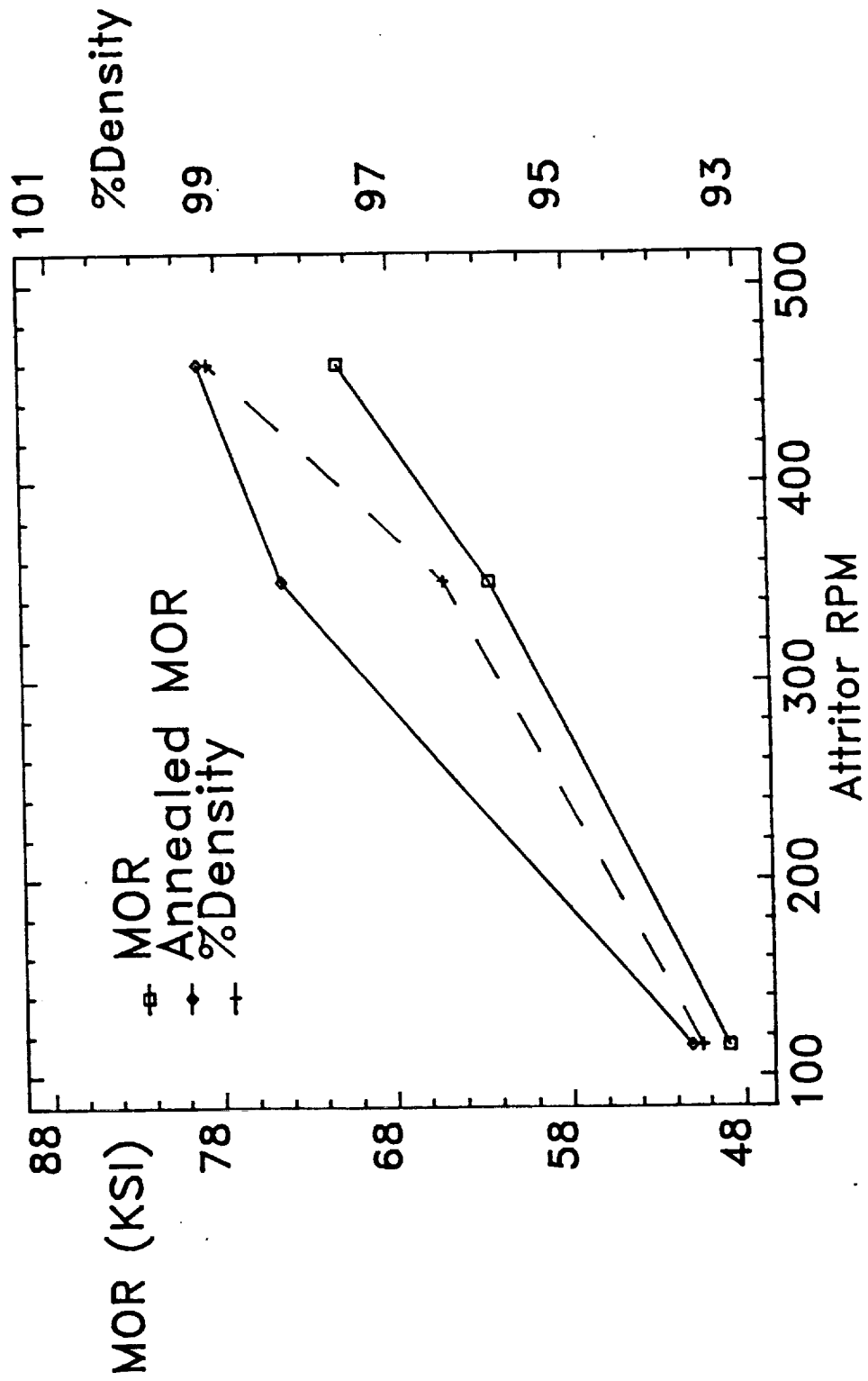


FIGURE 24

uniform level of homogeneity with increasing rotational speed.

This important correlation between mixer speed and strength was used to meet the goals of the program.

3. TASK III MOR (MODULUS OF RUPTURE) OPTIMIZATION

3.1 Experimental Plan

The plan was to select the best composition and process from the results of the Task II - Matrix 2 study and the Task VII - Matrix 12 (Attritor Speed Optimization) study and prepare 3 duplicate batches of material. All of the bars would be annealed, one-half of the bars would be hipped and a proof testing experiment to improve the Weibull modulus would be performed on the strongest group (annealed or HIPped). The goals of the experiment were to reach or exceed the goals of the program, which are a Weibull characteristic strength of at least 550 MPa (80 Ksi) and a Weibull modulus of 16.

3.1.1 Sample Preparation

The composition selected from the Task II - Matrix 2 experiment was 2.6% carbon as carbon black, 0.4% boron as amorphous boron and 97% SiC UF Ibiden powder. Each batch was fluid mixed with toluol in an attritor mixer at 460 rpm. Each of the 3 batches (A, B, and C) provided 225 molded bars, of which 120 were dewaxed and sintered, and 60 of the sintered bars were HIPped. All of the 120 bars from each batch were machined and annealed. Thirty of each batch were tested in the HIPped-machined-annealed condition, 30 in the machined-annealed condition and 60 in the machined-annealed-proof tested condition. The sintering conditions were those determined from Task VII - Matrix 8 (Ref. 3). The HIP conditions were 207 MPa (30 Ksi) argon pressure at 1950⁰ C for 30 minutes. The annealing conditions were 1200⁰ C for 18 hr. in air.

3.1.2 Analysis of Data and Discussion of Results

Density Data

A summary of the density data, mean and standard deviation, are shown in Table XIV. Although all densities are high and acceptable for high strength, both the molded and the sintered densities of batch A are below the densities of the other two batches. The correlation of molded density and water vapor in the air, observed earlier in this program (Ref. 2), appears to be present for these data, since the amount of water in the environmental air during molding was the highest for batch A.

Strength Data

An initial group of approximately 30 MOR bars from each of A, B, and C batches in both the machined-annealed and the HIP-machined annealed conditions were evaluated for strength. The results are summarized in Table XV. The HIP bars are lower in strength for each of the batches, and the strength values, grouped for all batches, are significantly lower for the HIP material. Microstructural observations on the HIP bars indicate

TABLE XIV

DENSITY OF TASK III MATERIALS

	<u>BATCH A</u>		<u>BATCH B</u>		<u>BATCH C</u>	
	<u>\bar{X}</u>	<u>S</u>	<u>\bar{X}</u>	<u>S</u>	<u>\bar{X}</u>	<u>S</u>
Mold g/cc	2.2622	0.012	2.2808	0.006	2.2767	0.007
Sint g/cc	3.1262	0.003	3.1335	0.002	3.1360	0.003
Sint % TD	98.6		98.8		98.8	

Sample size = 120 for each batch

TABLE XV

EFFECT OF HIP ON STRENGTH (KSI)
DATA FROM TASK III

<u>BATCH</u>	<u>n</u>	<u>\bar{x}</u>	<u>S</u>	<u>θ</u>	<u>m (MLE)</u>
A	30	82.5	13.9	88.1	7.0
A HIP	30	77.9	11.8	82.6	7.8
B	30	81.3	15.1	87.4	6.3
B HIP	30	76.3	12.6	81.7	7.2
C	29	82.3	12.3	87.1	7.9
C HIP	29	76.9	14.0	82.5	6.4

n = number of samples

\bar{x} = mean MOR

S = standard deviation

θ = Weibull characteristic strength

m = Weibull modulus, Max. Likelihood Est.

some grain growth had occurred during the HIP process and this may explain the lower strength. From these results it was decided to select the large MOR groups and the proof tested groups from material which were not subjected to the HIP process.

A summary of the strength data from Task III is given in Table XVI with 60 samples tested from each of the 3 batches and the normal distribution parameters (mean and standard deviation) and the Weibull distribution parameters (characteristic value and modulus) listed in the Table. The data are given under two headings; all data are presented in one column and data with outliers (values way beyond the expected values of the distribution) removed are given in the second column. Boxplot exploratory analysis, normal probability plots, and a test commonly used for outliers in data sets (Ref. 8) were used to point out the outliers. One outlier was found in each of batches A and B, and two outliers were present in C. The outliers influenced the location parameter, mean or characteristic value, a small amount, but had a larger influence on the scale parameter (standard deviation and Weibull modulus). The proof tested group and the group tested at 1400⁰ C had no outliers.

The data presented in Table XVI clearly show that the strengths exceed 550 MPa (80 Ksi) in all instances for the Weibull characteristic value and in all but two instances for the mean strength. The 1400⁰ C strength is the same as the room temperature strength.

The proof tested group was subjected to a proof test of 586 MPa (85 Ksi) prior to testing at room temperature (Ref. 9). This led to a truncated distribution of the strength of the bars as shown in the probability density distribution in Figure 25 and in the cumulative distribution in Figure 26. The group of 70 bars from the 3 batches had a mean strength of 635 MPa (92.2 Ksi), a Weibull characteristic strength of 655 MPa (95.0 Ksi), a standard deviation of 38 MPa (5.6 Ksi), and a Weibull modulus of between 15.7 and 18.4.

The Weibull modulus can be estimated in several ways, the most common are the maximum likelihood estimation (MLE) and the least squares estimation (LSE) (Ref. 10). The data groups in Task III were used to calculate the Weibull modulus using both the MLE and LSE methods. Table XVII contains a comparison of the two methods for the groups of data, with and without outliers, within Task III. The R^2 Adj. (Ref. 11) can be considered as a measure of the goodness of fit of a least squares regression line to the data. Box and Cox transformations (Ref. 4) of the data led to very high values of R^2 Adj. One can see from the data that the MLE and the LSE estimates are in close agreement for the three batches. The removal of the outliers in the data increases the Weibull modulus by about 0.7. The close agreement between MLE and LSE implies that the error term in the least squares model is for errors that are normally and independently distributed (Ref. 13). Since we attribute the variance in the data to the flaw distribution in the samples, we can assume that the flaws are normally and independently distributed.

The modulus determined for the group that was proof tested at 570 MPa (83 Ksi) is somewhat meaningless since the truncated distribution formed by the proof testing process is not a Weibull distribution. The MLE and the

TABLE XVI

SUMMARY OF STRENGTH DATA FROM TASK III

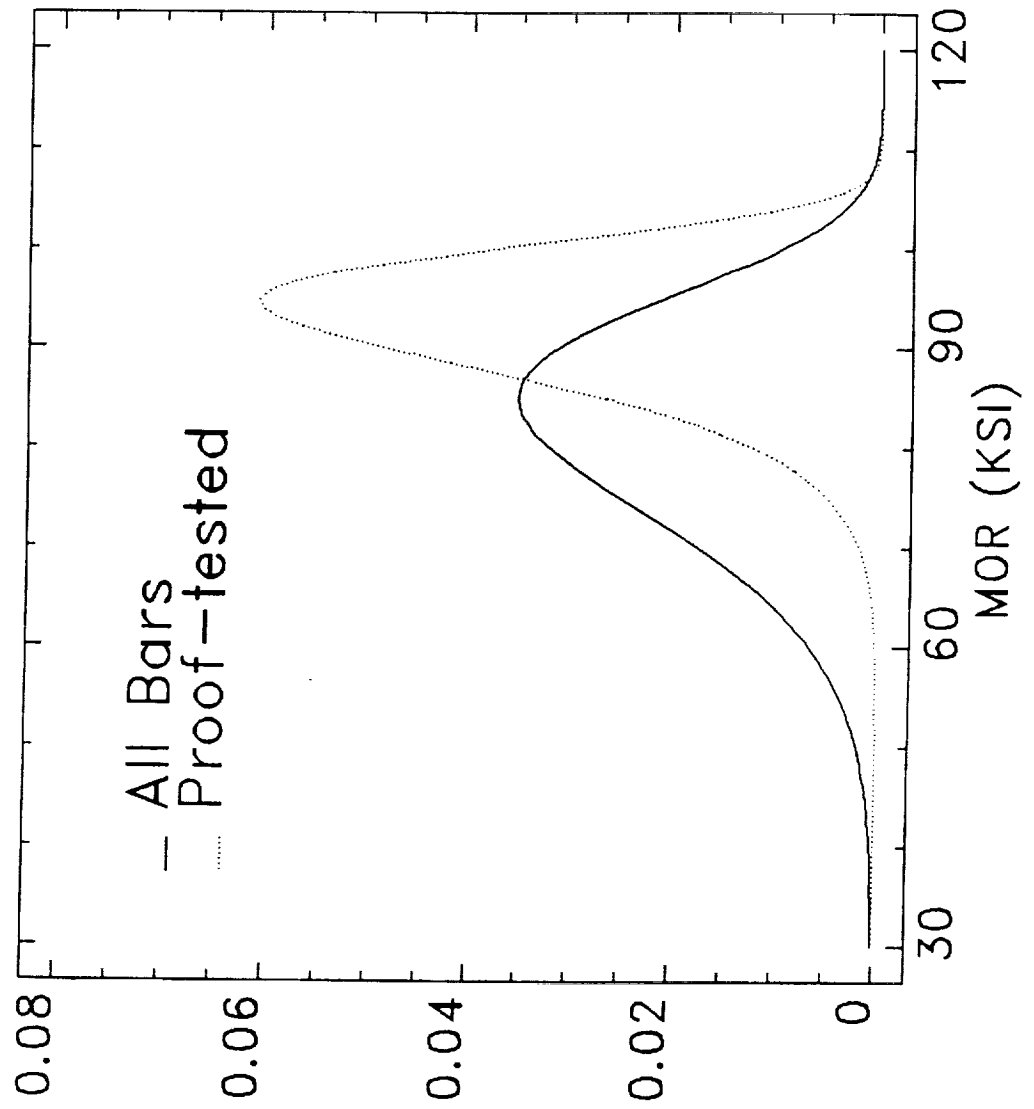
BATCH	ALL DATA					WITHOUT OUTLIERS				
	<u>n</u>	<u>\bar{x}</u>	<u>S</u>	<u>θ</u>	<u>m</u>	<u>n</u>	<u>\bar{x}</u>	<u>S</u>	<u>θ</u>	<u>m</u>
A	60	80.8	12.3	85.9	7.6	59	81.5	11.2	86.4	8.0
B	60	79.7	11.3	84.2	8.6	59	80.4	9.9	84.7	9.2
C	60	83.9	11.6	88.7	8.5	58	85.1	9.9	89.4	9.2
ABC	180	81.5	11.8	86.3	8.2	176	82.3	10.5	86.9	8.7
PT	70	92.2	5.6	95.0	15.7					

TESTED AT 1400 C

ABC	16	83.7	11.1	88.1	9.0
ABC*	16	78.7	10.7	83.0	8.8

- n = number of samples
- \bar{x} = mean MOR (KSI)
- S = standard deviation
- θ = Weibull characteristic strength
- m = Weibull modulus
- * = HIP'D samples

Task III Weibull Probability Density Function



Task III Weibull Cumulative Distribution Function

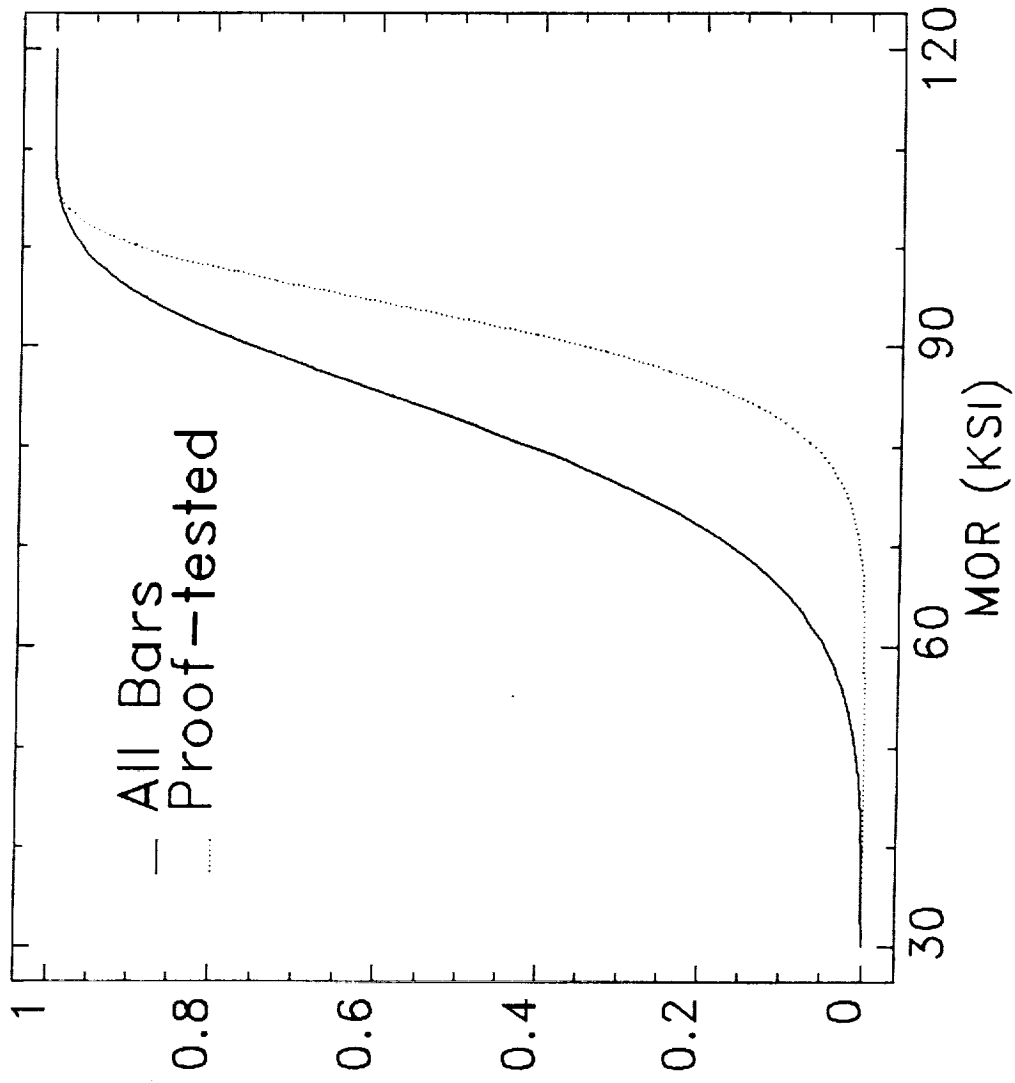


FIGURE 26

TABLE XVII

TASK III

COMPARISON OF WEIBULL MODULUS
CALCULATED BY MLE AND LSE METHODS

<u>BATCH</u>	<u>n</u>	<u>ALL DATA</u>			<u>n</u>	<u>WITHOUT OUTLIERS</u>		
		<u>(m)</u>		<u>(R² ADJ.)</u>		<u>(m)</u>		<u>(R² ADJ.)</u>
		<u>MLE</u>	<u>LSE</u>			<u>MLE</u>	<u>LSE</u>	
A	60	7.6	7.4	(97.1%)	59	8.0	8.1	(99.1%)
B	60	8.6	8.4	(96.9%)	59	9.2	9.0	(99.0%)
C	60	8.5	8.4	(98.0%)	58	9.2	9.6	(98.8%)
ABC	180	8.2	8.3	(98.9%)	176	8.7	9.0	(99.5%)
P.T.	70	15.7	21.9	(99.3%)				

P.T. = PROOF TESTED

LSE of the Weibull modulus is clearly different, indicating that the flaws are not normally or independently distributed. This is obvious from the way we have proof tested the samples since the weak samples have been removed from the population. The MLE of the Weibull modulus is the preferred value based on the desirable properties of maximum likelihood estimates (Ref. 10). The Weibull distribution of the 70 proof-tested bars is shown in Figure 27. One can see that the lower tail of the distribution departs from the MLE-estimated line.

The Weibull modulus data for Task III, and also for most of the other groups in this program, have remained fairly constant between 8 and 9 for large sample groups. This is consistent with the fact that the flaw distribution has remained constant although the strength of the material has been significantly improved (mean flaw size has decreased). Kendall and co-workers (Ref. 12) have shown both theoretically and experimentally that fracture toughness does not influence the Weibull modulus of bending strength for materials that obey the Griffith criterion for crack propagation. They have also shown for titanium dioxide that very weak, green materials have the same modulus as strong, sintered materials, since they have the same flaw size distribution. Only by changing the flaw size distribution by proof testing were we able to significantly change the Weibull modulus.

Fracture origins in MOR bars from Task III were not readily found because the high level of strength developed in these materials tends to destroy the surface during testing. A few surfaces were found and typical fracture surfaces and microstructures are shown in Figures 28 for a machined and annealed sample and in Figure 29 for a HIP-machined-annealed sample. Figure 28 clearly shows the surface initiated failure origin which appears to be a fine crack. The microstructure is similar to that seen previously and the fracture mode is transgranular. In the HIPed sample failure originated just below the tensile edge as seen in Figure 29. The fracture surface appears to be rougher, possibly due to some small increase in SiC grain size. The increased grain growth may be related to the HIP process which included heating at 1950⁰ C for 30 minutes.

Task III: Proof-tested

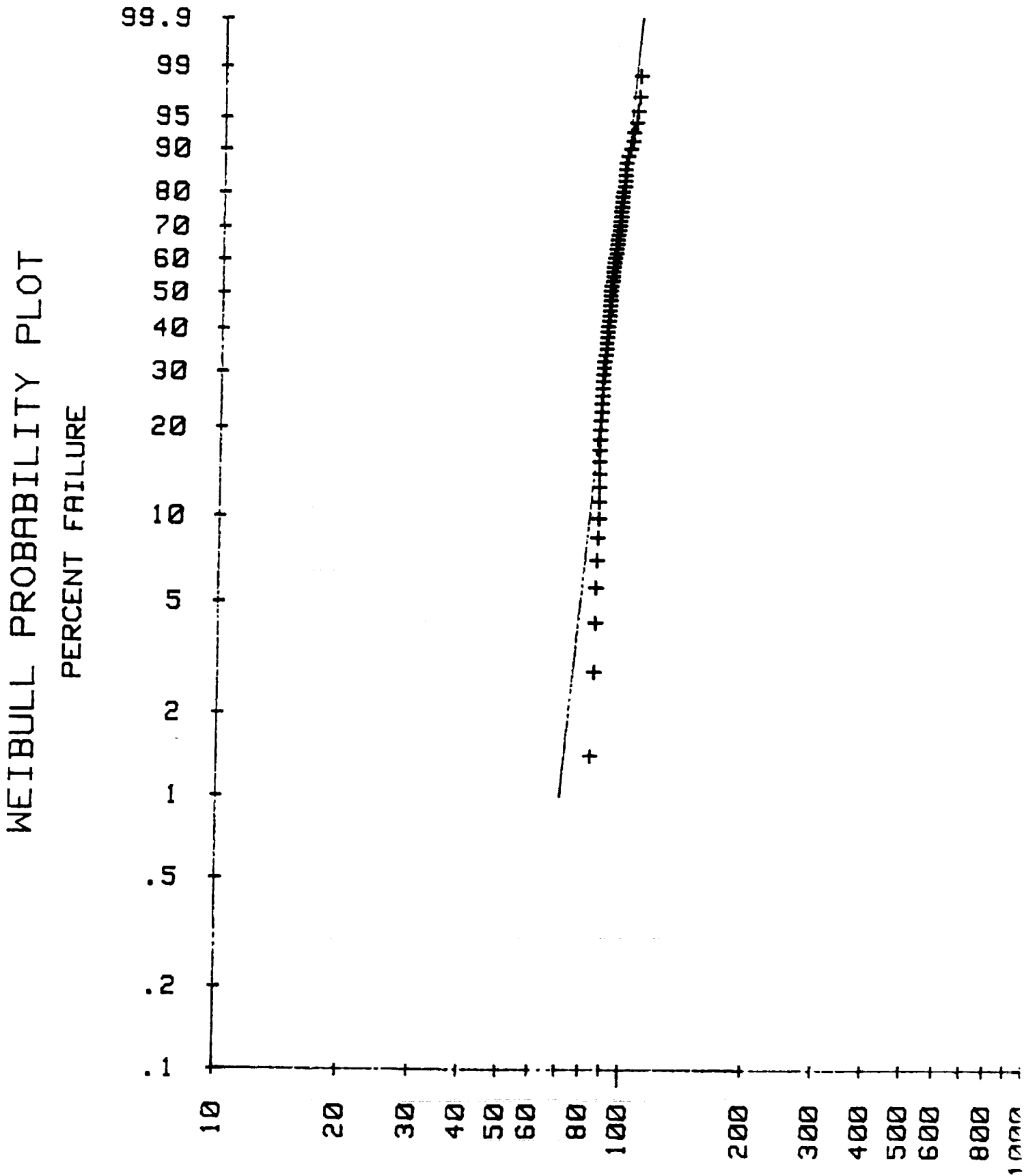


FIGURE 27

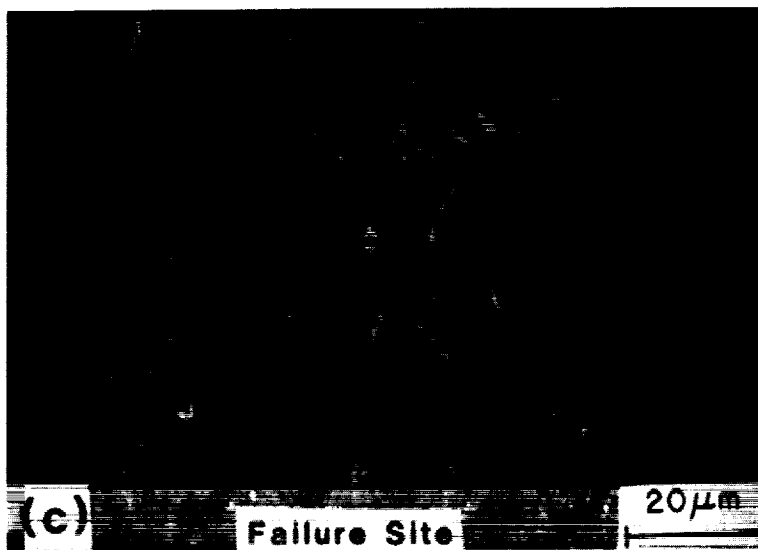
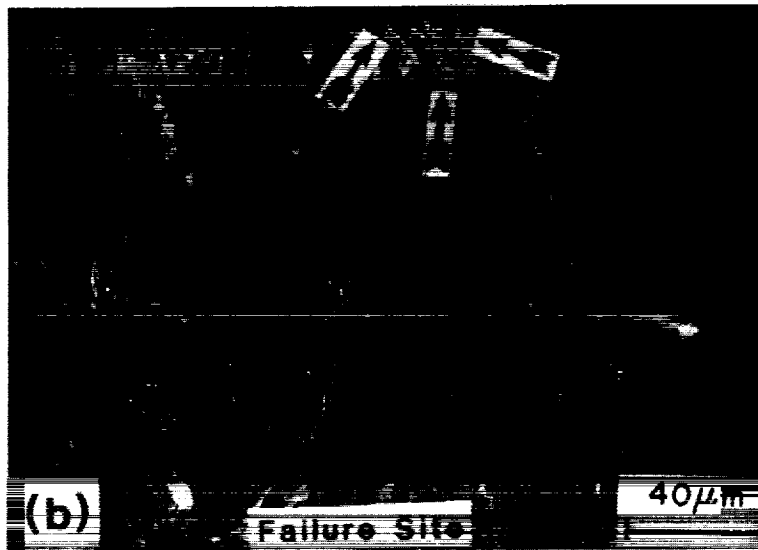
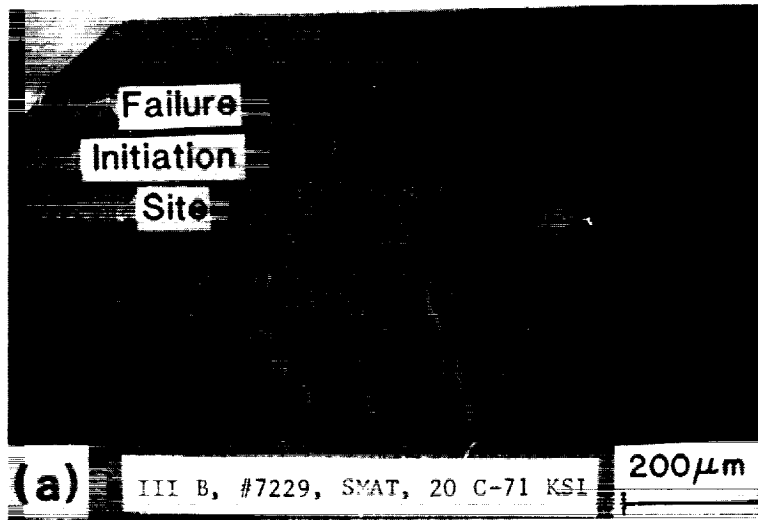
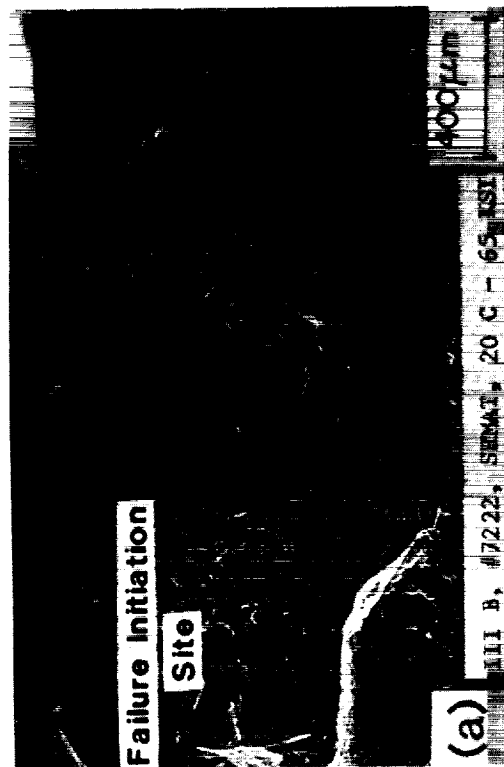


FIGURE 28



CONCLUSIONS

Strength improvements in injection-molded, pressureless-sintered SiC were attained by using statistically-designed experiments to investigate processing and composition variables which led to the reduction of flaw size in these materials. Weibull characteristic strengths above 550 MPa (80 Ksi) and Weibull modulus of 16, which were the goals of this program, were achieved. The program resulted in an increase of 87% in MOR bar Weibull strength and, by proof testing, a 100% increase in Weibull modulus over the values developed in the baseline material.

Sintered densities were improved from 94% of theoretical density to 99% in the sintered material (and 100% in the HIP material).

Flaw sizes were reduced from about 100 microns in the baseline material to about 10 microns in the Task III material.

A fluid mixing process with an attritor mixer was developed which provided material with the highest strength. The speed of the attritor was found to be an important variable in the process.

Sintering cycle parameters were improved by using two-level factorial experiments and introducing both vacuum and argon environments during the cycle.

Annealing of machined MOR bars in air significantly increased the strength.

Strength measurements at 1200⁰ C and 1400⁰ C were the same as those at room temperature. These materials may be the strongest, stable materials known at 1400⁰ C in air, which are capable of being formed into complex parts.

The number of flaws per bar observed visually and by X-ray analysis in molded and sintered bars were observed to follow a Poisson distribution, and the number of flaws in molded bars is drastically reduced by sintering.

Statistical process control was found to be useful in the mixing, molding, dewaxing and sintering processes.

Although the location factor in the Weibull distribution (characteristic strength) was significantly increased during the program by improved processing procedures and composition, the scale factor (Weibull modulus) remained essentially constant with these improvements. The present level of development of the material and process yielded modulus values of approximately 8 to 9 for large sample sizes, and only by truncating the strength distribution with proof testing was it possible to improve the modulus to 16. The constant modulus value implies that the distribution of flaws is constant, although the mean flaw size has been drastically reduced during this work. Since the maximum likelihood and the least squares estimators of the Weibull modulus gave the same values, it is implied that the flaws are independently and normally distributed in the

samples. Higher modulus values may be possible by clean-room procedures which may truncate or narrow the flaw size distribution prior to testing.

It has been the experience during this program that the data on strength and density of MOR bars can be adequately represented by a normal distribution and normal statistical tests are valid. With large sample sizes (>30 bars) a Weibull distribution may be adequate, but should be tested in each case. Outliers have usually been found in data sets of strength and, on the average, 2 bars per 100 are outliers for normal, or Weibull, distribution, regardless of considerable efforts to perform nondestructive tests.

It has been shown that proof testing can provide improved reliability in the form of increased Weibull modulus or decreased standard deviation.

Hot isostatic pressing improved the strength of material at strength levels below about 480 MPa (70 Ksi), but did not improve strength at levels beyond that strength, as in Task III materials.

Magic angle spinning nuclear magnetic resonance was found to be a powerful tool in determining the silicon carbide polytypes present in both the starting powders and the sintered samples.

REFERENCES

1. T. J. Whalen and W. L. Winterbottom, "Improved Silicon Carbide for Advanced Heat Engines", NASA Contractor Report 179477, September, 1986.
2. Thomas J. Whalen, "Improved Silicon Carbide for Advanced Heat Engines", NASA Contractor Report 180831, October, 1987.
3. Thomas J. Whalen, "Improved Silicon Carbide for Advanced Heat Engines: Third Annual Report", NASA Contractor Report 182186, August, 1988.
4. G. E. P. Box, W. G. Hunter and J. S. Hunter, Statistics for Experimenters, John Wiley and Sons, New York, 1978.
5. Cuthbert Daniel, Applications of Statistics to Industrial Experimentation, John Wiley and Sons, New York, pp 22-28, 1976.
6. Douglas C. Montgomery, Design and Analysis of Experiments, Second Edition, John Wiley and Sons, New York, pp281-90, 1984.
7. G. R. Findlay, J. S. Hartman, M. F. Richardson and B. L. Williams, J. Chem. Soc., Chem. Comm., pp159 - 161, 1985.
8. David C. Hoaglin, Frederick Mosteller, and John W. Tukey, Understanding Robust and Exploratory Data Analysis, Chapter 2, John Wiley and Sons, New York, 1983.
9. J. E. Ritter Jr., P. B. Oates, E. R. Fuller Jr., S. M. Wiederhorn, J. of Materials Science, 15, 2272-2295, 1980.
10. A. M. Mood, F. A. Graybill and D. C. Boes, Introduction to the Theory of Statistics, Third Edition, McGraw-Hill Book Company, New York, 1974.
11. J. Neter, W. Wasserman and M. H. Kutner, Applied Linear Regression Models, R. C. Irwin, Inc., Homewood, Illinois, 1983.
12. K. Kendall, N. McN. Alford, S. R. Tan, and J. D. Birchall, J. Mater. Res., 1 (1) 120, 1986.
13. G. E. P. Box, N. R. Draper Empirical Model-Building and Response Surfaces, John Wiley and Sons, New York 1987.



Report Documentation Page

1. Report No. NASA CR-182289	2. Government Accession No.	3. Recipient's Catalog No.	
4. Title and Subtitle Improved Silicon Carbide for Advanced Heat Engines	5. Report Date May 1989		
	6. Performing Organization Code		
7. Author(s) Thomas J. Whalen	8. Performing Organization Report No. None		
	10. Work Unit No. 505-63-1A		
9. Performing Organization Name and Address Ford Motor Company P.O. Box 2053 Dearborn, Michigan 48121-2053	11. Contract or Grant No. NAS3-24384		
	13. Type of Report and Period Covered Contractor Report Final		
12. Sponsoring Agency Name and Address National Aeronautics and Space Administration Washington, D.C. 20546-0001	14. Sponsoring Agency Code		
	15. Supplementary Notes Project Manager, Nancy J. Shaw, Materials Division, NASA Lewis Research Center.		
16. Abstract This is the final technical report for the program entitled "Improved Silicon Carbide for Advanced Heat Engines" for the period February 12, 1985 to December 11, 1988. The objective of the program was the development of high strength, high reliability silicon carbide parts with complex shapes suitable for use in advanced heat engines. Injection molding was the forming method selected for the program because it is capable of forming complex parts adaptable for mass production on an economically sound basis. The goals of the program were to reach a Weibull characteristic strength of 550 MPa (80 ksi) and a Weibull modulus of 16 for bars tested in four-point loading. Statistically-designed experiments were performed throughout the program and a fluid mixing process employing an attritor mixer was developed. Compositional improvements in the amounts and sources of boron and carbon used and a pressureless sintering cycle were developed which provided samples of about 99 percent of theoretical density. Strengths were found to improve significantly by annealing in air. Strengths in excess of 550 MPa (80 ksi) with Weibull modulus of about 9 were obtained. Further improvements in Weibull modulus to about 16 were realized by proof testing. This is an increase of 86 percent in strength and 100 percent in Weibull modulus over the baseline data generated at the beginning of the program. Molding yields were improved and flaw distributions were observed to follow a Poisson process. Magic angle spinning nuclear magnetic resonance spectra were found to be useful in characterizing the SiC powder and the sintered samples. Turbocharger rotors were molded and examined as an indication of the moldability of the mixes which were developed in this program.			
17. Key Words (Suggested by Author(s)) Silicon carbide; Injection molding; Nonoxide ceramics; Sintering; Statistically designed experiments; Factorial experiments; Flaw distribution; Hipping; Poisson process; Weibull statistics; Magic angle spinning nuclear magnetic resonance			
Date for general release <u>May 1991</u> Subject Category <u>27</u>			
19. Security Classif. (of this report) Unclassified	20. Security Classif. (of this page) Unclassified	21. No of pages 60	22. Price* A04

